NLR Nod1 signaling promotes survival of BCR-engaged mature B cells through up-regulated Nod1 as a positive outcome

Kyoko Hayakawa,[1] Anthony M. Formica,[1] Yan Zhou,[1] Daiju Ichikawa,[1] Masanao Asano,[1] Yue-Sheng Li,[1] Susan A. Shinton,[1] Joni Brill-Dashoff,[1] Gabriel Núñez,[2] and Richard R. Hardy[1]

[1]Fox Chase Cancer Center, Philadelphia, PA
[2]Department of Pathology and Comprehensive Cancer Center, University of Michigan Medical School, Ann Arbor, MI

Although B cell development requires expression of the B cell antigen receptor (BCR), it remains unclear whether engagement of self-antigen provides a positive impact for most B cells. Here, we show that BCR engagement by self-ligand during development in vivo results in up-regulation of the Nod-like receptor member Nod1, which recognizes the products of intestinal commensal bacteria. In anti-thymocyte/Thy-1 autoreactive BCR knock-in mice lacking self–Thy-1 ligand, immunoglobulin light chain editing occurred, generating B cells with up-regulated Nod1, including follicular and marginal zone B cells with natural autoreactivity. This BCR editing with increased Nod1 resulted in preferential survival. In normal adult mice, most mature B cells are enriched for Nod1 up-regulated cells, and signaling through Nod1 promotes competitive survival of mature B cells. These findings demonstrate a role for microbial products in promoting survival of mature B cells through up-regulated Nod1, providing a positive effect of BCR engagement on development of most B cells.

INTRODUCTION

Although appropriate T cell antigen receptor binding to self-ligands is a well-documented step in T cell maturation known as "positive selection"(Klein et al., 2009), a positive role for self-ligand engagement by the majority of B cells remains unclear. In mice, the majority of mature B cells form follicles in the lymphoid organs, hence their name, follicular (FO) B cells. Prior work has demonstrated that B cell antigen receptor (BCR) expression is essential for the survival of B cells (Kraus et al., 2004), and delivery of a "tonic" BCR signal in the absence of BCR ligand engagement is sufficient for progression to mature FO B cells (Pelanda et al., 1997; Rowland et al., 2010). In this process, availability of the tumor necrosis factor member BAFF (B cell activating factor), provided mainly by myeloid and stromal cells in the microenvironment, is critical for allowing mature B cell survival (Mackay and Schneider, 2009; Mackay et al., 2010).

Although maturation can occur without BCR ligand when BAFF is provided, self-antigen–dependent positive selection is known to occur for two minor B cell subsets in mice, B1 B (Hayakawa et al., 1999) and marginal zone (MZ) B cells (Martin and Kearney, 2000; Wen et al., 2005a). Both of these subsets contain autoreactive B cells that produce autoantibodies (Hayakawa et al., 1999; Wen et al., 2005a; Baumgarth, 2011; Ichikawa et al., 2015). Though B1 B cells are dominantly generated in early life as a unique Lin28$^+$ fetal/neonatal B-1 development outcome (Yuan et al., 2012; Zhou et al., 2015), MZ B cells are generated from BM through Lin28$^-$ B-2 development after the neonatal stage. In adults, FO B cells are the major mature IgM$^{med/low}$IgD$^+$ B cell type from B-2 development, and most have no clearly detectable autoreactivity. However, some FO B cells show autoreactivity, and mutations that handicap NF-κB activation induced by BCR signaling result in a decreased frequency of FO B cells, in particular IgM^{lo}IgD$^+$ FO B cells, together with a severe reduction of B1 B and MZ B cells (Thome, 2004). Furthermore, a large fraction of the FO B cell pool expresses Nur77, a gene rapidly up-regulated by BCR ligand signaling from the transitional stage, but not in B cells, where the BCR ligand is absent, and IgM^{lo}IgD$^+$ B cells express the highest levels of Nur77 among FO B cells, suggesting that antigen-experienced cells predominate in the FO B subset (Zikherman et al., 2012). Recent data indicate that IgD

Correspondence to Kyoko Hayakawa: kyoko.hayakawa@fccc.edu

D. Ichikawa's present address is Division of Clinical Physiology and Therapeutics, Keio University Faculty of Pharmacy, Tokyo, Japan.

M. Asano's present address is Dept. of Internal Medicine and Rheumatology, Juntendo University School of Medicine, Tokyo, Japan.

Y.-S. Li's present address is DNA Sequencing and Genomic Core, National Heart, Lung, and Blood Institute, National Institutes of Health, Bethesda, MD.

Abbreviations used: AGcA, anti-intestinal goblet cell autoreactive; AGcAμκTg, V_H3609μ/$V_κ$19-17κ transgenic; ATA, anti-thymocyte/Thy-1 autoreactive; ATAid^{lo}, a higher ratio of kappa to ATA idiotype fluorescence staining intensity; ATAμκTg, V_H3609μ/$V_κ$21-5κ transgenic; B1a, CD5$^+$ B1 B; BAFF, B cell activating factor; BCR, B cell antigen receptor; CiE-DAP, C12-iE-DAP; FO, follicular; MZ, marginal zone; PerC, peritoneal cavity; Thy^{KO}, Thy-1 knockout; Thy^M, thymocyte plasma membrane; Thy^{WT}, normal wild-type self–Thy-1; V_H3609t × V_t21-5Tg, V_H3609/D/J_H2 knock-in mice crossed with $V_κ$21-5κ transgenic mice.

The Rockefeller University Press
J. Exp. Med. 2017 Vol. 214 No. 10 3067–3083
https://doi.org/10.1084/jem.20170497

BCRs require polyvalent antigens for activation, whereas they are unresponsive to monovalent antigens, in contrast with IgM BCRs (Übelhart et al., 2015). These data argued that the majority of $IgM^{med/low}IgD^{+}$ FO B cells have experienced some level of BCR engagement, with a different extent and form of engagement. However, it remained unclear whether the BCR ligand engagement experience has a positive impact on FO B cells compared with ligand ignorance.

BCR deletion or BCR editing accomplished mainly by further rearrangement of the Ig light chain (IgL) locus (Wardemann et al., 2003, 2004; Halverson et al., 2004; Nemazee, 2006) was originally described as a major negative selection mechanism that eliminates dangerous autoreactive specificities during mature B cell generation. However, BCR editing also occurs in B cells that lack self-reactivity (Cascalho et al., 1997; Braun et al., 2000), for reasons that have been debated, arguing against an exclusive role in negative selection but, alternatively, the possibility of positive selection. Here, we show that L chain editing occurs in an anti-thymocyte/Thy-1 BCR knock-in mouse model lacking self-Thy-1 ligand, resulting in preferential survival of BCR edited B cells, including FO B and MZ B cells with natural autoreactivity, and $IgM^{lo}IgD^{+}$ FO B cells predominantly composed of edited B cells. Generation of mature B cells via BCR editing in this model is associated with up-regulation of the NOD (nucleotide-binding oligomerization domain)–like receptor (NLR) Nod1. Nod1 recognizes the iE-DAP (γ-D-glutamyl-*meso*-DAP) dipeptide found in peptidoglycan present in the cell wall of gram-negative commensal gut microbiota (Chamaillard et al., 2003). A portion of this DAP-containing bacterial product is constantly turned over and translocated from the intestine into the circulation (Clarke et al., 2010), thereby providing a continual signal and competitive survival advantage for BCR-engaged mature B cells.

RESULTS

ATA B cells in the absence of self-antigen undergo BCR editing

BCR with $V_H3609/D/J_H2$ μ heavy chain together with $V_k21\text{-}5/J_k2$ κ light chain expression (as $V_H3609\mu/V_k21\text{-}5\kappa$) recognizes a Thy-1/CD90 glycoform predominantly expressed by immature thymocytes and also secreted in serum (Hayakawa et al., 1999; Wen et al., 2005a). As previously shown (and summarized in Fig. 1), expression of $V_H3609\mu/V_k21\text{-}5\kappa$ at the immature stage drives positive selection of B cells as anti-thymocyte/Thy-1 autoreactive (ATA) B cells in the presence of normal WT self–Thy-1 (Thy^{WT}; Hayakawa et al., 1999). Such ATA B cells, which induce CD5 as B1a ($CD5^{+}$ B1 B), are largely the product of fetal/neonatal B cell development (B-1), constituting a minor B cell subset in adults, as B1 B cells (Hardy and Hayakawa, 2001). This ATA B cell positive selection is independent of CD40-signal and does not require mature T cells (Hayakawa et al., 2016). In adult B cell development (B-2) from BM, expression of $V_H3609\mu/V_k21\text{-}5\kappa$ BCR drives negative selection, resulting in arrest. However, when $V_H3609\mu$ cells express $V_k19\text{-}17/J\kappa1$ light chain (as $V_H3609\mu/V_k19\text{-}17\kappa$), the generation of MZ B dominates, and some FO B cells are also generated. This BCR is a natural anti-intestinal goblet cell autoantibody (AGcA) binding to the mucin 2 glycoprotein (Ichikawa et al., 2015). This positive outcome of autoreactive BCRs by B1a, MZ B, and some FO B cells was confirmed in V_H3609 Igμκ transgenic mice (Hayakawa et al., 1999) and also the $V_H3609/D/J_H2$ targeted insertion (knock-in) mouse line V_H3609t (Ichikawa et al., 2015). Generation of ATAμκ transgenic (ATAμκTg) mice, allowing a dominant presence of $V_H3609\mu/V_k21\text{-}5\kappa$ ATA B cells at the immature B cell stage, provided the evidence that ATA B cells mature as FO B cells in the absence of self–Thy-1 in Thy-1–knockout mice (Thy^{KO}), in contrast to their arrest under Thy^{WT} (Hayakawa et al., 2003; Fig. 1).

In ATAμκ Tg mice, ATA B cells dominantly mature under Thy^{KO}, without BCR editing. However, this ATAμκ transgene was made without addition of the Igδ-constant region (Cδ), thus lacking ATA IgD. To further assess the fate of ATA B cells from adult B cell development, a $V_H3609/D/J_H2$ knock-in mouse line, V_H3609t, allowing IgD generation, was crossed with $V_k21\text{-}5\kappa$ L chain transgenic mice. This $V_H3609t \times V_k21\text{-}5$Tg mouse also generated an initial predominance of B cells with the complete ATA BCR in the immature BM B cell pool (Fig. 2 A). As expected, these $V_H3609t \times V_k21\text{-}5$Tg mice ($V_H3609^{+/-}V_k21\text{-}5^{+/-}$) accumulated ATA B cells in neonates that were present in the adult peritoneal cavity (PerC) as B1a with $IgM^{+}IgD^{lo/-}$ under a normal background (Thy^{WT}; Fig. 2 A, PerC) and showed progressively increased ATA serum levels with age (Fig. 2 B), as found in V_H3609t mice (Fig. S1). In the same adult mice, spleen B cells, predominantly as an outcome of B-2 development, showed a developmental arrest by ATA B cells (Fig. 2 A, red diagonal region) at the T2 transitional stage ($AA4/CD93^{+}CD23^{+}$) under Thy^{WT} condition, with down-regulation of surface IgM and IgD, as a result of negative selection. In the absence of self-antigen (Thy^{KO}), ATA BCR^{+} cells became mature B cells ($AA4^{-}$ $CD23^{+}$) with an IgM^{med}/IgD^{+} phenotype. These ATA B cell data confirmed negative selection by the presence of a self-antigen and B cell maturation by BCR tonic signaling as previously found in ATAμκ transgenic mice. Surprisingly, however, the $IgM^{lo}IgD^{+}$ FO B cell compartment in the absence of Thy-1 antigen was predominantly composed of BCR-edited B cells (Fig. 2 A, Thy^{KO}). This editing was accelerated under Thy^{WT} conditions (Figs. 2 A and S2 A). As shown in Fig. 2 C, in the spleen of Thy^{KO} mice, ATA B cells predominated at the $AA4^{+}$ transitional stage, whereas $AA4^{-}$ mature B cells showed an increased number of cells with a higher ratio of kappa to ATA idiotype fluorescence staining intensity ("$ATAid^{lo}$" cells). These $ATAid^{lo}$ cells used the VDJ engineered chromosome (IgM^{a+}), and most retained the J_H-targeted VDJ (they are $V_H3609id^{+}$); however the BCRs in many B cells paired this engineered heavy chain with an endogenous Igκ L chain while still retaining the transgenic light chain at low levels on the surface, yielding $ATAid^{lo}$ cells

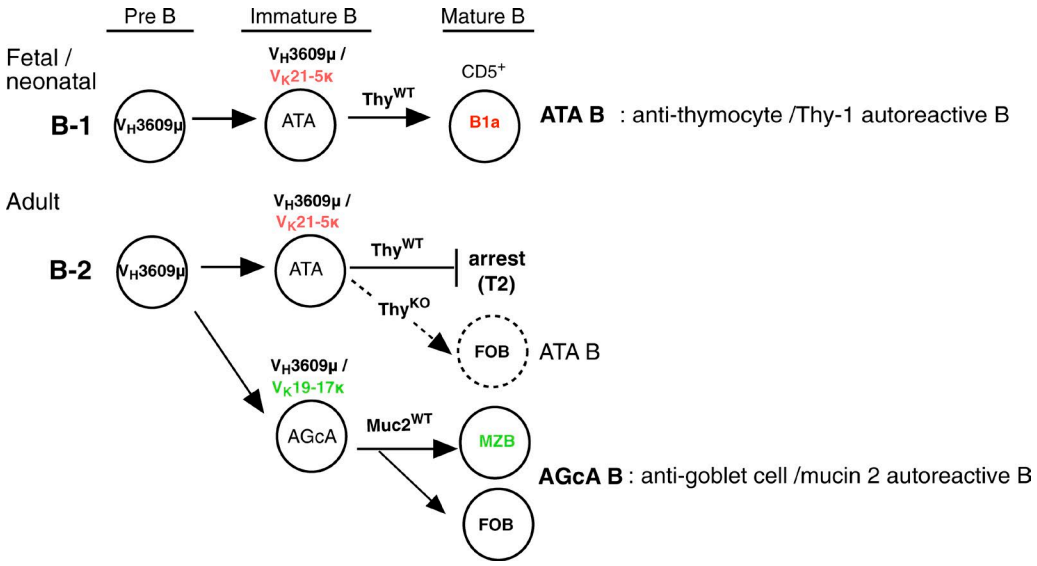

Figure 1. **Summary of autoreactive ATA B and AGcA B cell generation.** ATA B cell positive selection occurs from fetal/neonatal B-1 development to generate $CD5^+$ B cells as B1a, whereas negative selection (arrest) occurs during adult B-2 development. However, B-2 development allows generation of the autoreactive AGcA BCR (dominantly reactive to mucin 2), expressing different light chain from the ATA BCR, to dominantly become MZ B cells, and some also become FO B cells as mature B cells. Absence of self–Thy-1 antigen (Thy^{KO}) allows ATA B cell maturation to generate FO B cells from B-2 development. Following analysis, VDJ of $V_H3609µ$ ($V_H3609/D/J_H2$-µ) was as $V_H3609id$ ($V_H3609/D/J$ idiotype), $V_H3609µ/V_k21$-5κ ATA BCR was as ATAid (ATA idiotype). To detect $V_H3609µ/V_k21$-5κ ATA BCR, rat P9-19A4 antibody was used to recognize this ATAid BCR.

(Fig. 2 C, center; Table S1, Igκ usage; Fig. S3, endogenous and Tg Igκ coexpression). These L chain–edited B cells became either FO B or MZ B cells in the presence or absence of Thy-1 (Fig. 2 C, right, Thy^{KO}; and Fig. S2 A, Thy^{WT}). Significantly, L chain sequence analysis of the $ATAid^{lo}$-edited FO B cell population revealed inclusion of B cells with a natural autoreactive AGcA specificity ($auto^+$) by expression of a V_k19-17/J_k1 light chain paired with the V_H3609 heavy chain. This $auto^+$AGcA B generation was strongly represented in L chain–edited B cells in both $V_H3609t \times V_k21$-5Tg and ATAµκTg mice on a Thy^{WT} background as an outcome of negative selection (Fig. S3). Under Thy^{KO} conditions in $V_H3609t \times V_k21$-5Tg mice, AGcA B cell generation was also found in the edited FO B cell pool (3/23 [13%]; Fig. 2 D and Table S1) and further increased in MZ B cells.

This observation raised the possibility that B cell editing might involve a BCR ligand–mediated signal, even on a Thy^{KO} background. To identify genes altered between unedited ATA FO B and both edited and WT FO B cells, we performed a microarray analysis comparing these FO B cells. In parallel, FO B cells expressing $auto^-$ ATA in ATAµκTg. Thy^{KO} versus $auto^+$ AGcA in AGcAµκTg mouse lines (Ichikawa et al., 2015) were also compared. As shown in Table S2, our microarray results consistently revealed up-regulation of the NLR family member Nod1 in the edited B cell pool and $auto^+$ AGcA B cells, reaching a level similar to that in WT FO B cells, as confirmed by quantitative PCR, including the $ATAid^{lowest}$ cells (Fig. 2 E). In contrast, we observed no alteration of BAFF-R or TLR (TLR2, TLR4, TLR7, and TLR9) mRNA levels (not depicted). To assess the frequency of Nod1 up-regulated cells among edited B cells, we applied a flow cytometry assay, stimulating cells with Nod1 ligand (C12-iE-DAP [CiE-DAP]) in vitro and then assessing expression of the early activation marker CD69 6 h after stimulation (Fig. 2 E). This analysis revealed that levels of Nod1-responding cells were higher in the majority of both WT FO B cells and edited B cells than in un-edited ATA B cells, as were with Nod1 mRNA levels, indicating Nod1 up-regulation by edited B cells. These unedited and edited FO B cells were equally functionally mature and capable of responding to anti–IgM stimulation (Fig. 2 E). Strikingly, the frequency of unedited ATA B cells in Thy^{KO} mice declined further with age, and edited B cells (and B cells expressing endogenous IgH chains) became predominant (Fig. 2 F), suggesting that edited B cells have a survival advantage.

Nod1 signal sensitivity increases in mature B cells with age

In normal WT mice, neonatal-generated B1a cells expressed up-regulated Nod1 mRNA (Fig. 3 A). During B-2 development from adult BM, Nod1 mRNA levels slightly increased from the transitional to mature FO B stages and progressively increased in MZ B cells. B1a cell Nod1 mRNA expression continued to be the highest (Fig. 3 A). In contrast to such mature B cell subsets in WT mice, mature ATA FO B cells in nonedited ATAµκTg.Thy^{KO} mice showed lower levels of both Nod1 mRNA and cytoplasmic protein (Fig. 3, A and B) and the lowest response to CiE-DAP stimulation (Fig. 3 C). Nod1 is a cytosolic protein containing a Card 4 domain that is

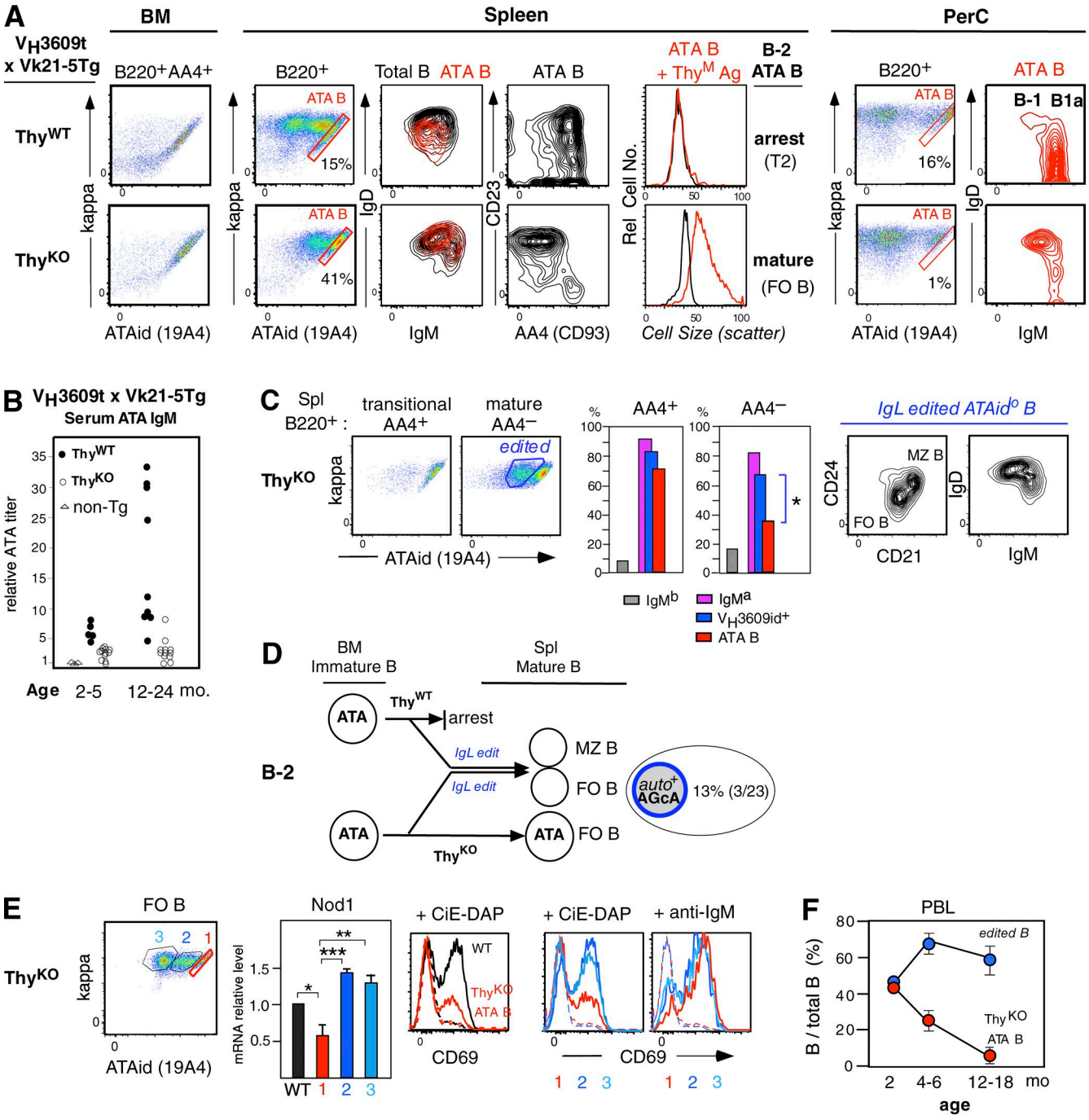

Figure 2. **BCR editing and Nod1 increase in mature B cells.** (A) B220$^+$ B cell analysis of V_H3609t knockout mice crossed with V_K21-5 Tg mice ($V_H3609^{+/-}V_K21\text{-}5^{+/-}$) on either Thy^{WT} or Thy^{KO} background. Gated unedited ATA B in the spleen and PerC (red diagonal, with percentage) for phenotype analysis, and in vitro 2 d Thy^M antigen stimulation outcome analysis with spleen ATA B. Thy^M, thymocyte plasma membrane (Hayakawa et al., 2003). PerC IgM$^+$IgD$^{lo/-}$ ATA B cells in Thy^{WT} were CD5$^+$ as B1a. (B) Relative ATA serum titer determined by a thymocyte staining assay. Nontransgenic CB17 mouse sera (at 1:100 dilution) was set to 1.0 as the staining background. (C) V_H3609t × V_K21-5 Tg.Thy^{KO} mouse spleen B cell analysis comparing transitional and mature B cells. Percentage of endogenous IgM (IgM^{b+}), VDJ engineered IgM (IgM^{a+}), VDJ-expressing B cells (V_H3609id$^+$), and unedited ATA B cells (ATAid^{hi}), out of total IgM (IgM^a + IgM^b). ATAid^{hi} B cell decrease with V_H3609id retention (center; n = 3; *, P < 0.01), generating L chain–edited ATAid^{lo} FO B and MZ B cells (right). (D) Auto$^+$ AGcA B cell presence in L chain–edited B cells, including in FO B cells under Thy^{KO} (Table S1). (E) In FO B cells under Thy^{KO}, ATA B (1) and edited B cell fractions (2 and 3) for Nod1 quantitative PCR analysis, together with WT FO B cells (n = 5; mean ± SE; *, P < 0.05; **, P < 0.005; ***, P < 0.001), and 6-h stimulation with CiE-DAP or anti-IgM. Unstimulated B cells shown as a dotted line. (F) Nonedited ATA B and edited B cell frequencies in total PBL B cells during aging in V_H3609t × V_K21-5 Tg.Thy^{KO} mice (n = 10–15 of each age group; mean ± SE).

found in diverse cell types (Fritz et al., 2006). Although Nod1 mRNA/protein levels are not substantially higher in FO B cells than other cell types in WT spleen, the majority of B cells in adult spleen showed sensitive activation responsiveness to CiE-DAP stimulation (Fig. 3 D). During normal mouse B cell maturation, a large fraction of mature cells became sensitive to CiE-DAP stimulation, with the greatest enrichment occurring among $IgM^{lo}IgD^{+}$ FO B cells (Fig. 3 E, top). These CiE-DAP–reactive mature FO B cells increased from young to older age (Fig. 3 F). In contrast to WT mice, the large reduction of FO B cell generation and a lack of $IgM^{lo}IgD^{+}$ B cells in Btk mutant *Xid* mice (Thomas et al., 1993) was associated with low Nod1 ligand responsiveness, and Nod1 mRNA remained low in aged *Xid* mice (Fig. 3 G). Collectively, these Nod1 data suggested the involvement of BCR signaling in Nod1 up-regulation and survival.

BCR-engaged B cells undergo Nod1 up-regulation

To test this concept, we first sought to verify whether ATA B cells under Thy^{KO} are capable of undergoing Rag (recombinase-activating gene)–dependent BCR editing at the transitional stage in the spleen. In WT mice, both Rag1 and Rag2 mRNAs (and proteins) are still detectable at the transitional stage, although at very low levels (Yu et al., 1999). This low level of Rag mRNA expression at the T1/T2 transitional stage was increased in ATA B cells under a Thy^{KO} compared with Thy^{WT} background in ATAμκTg mice (Fig. 4 A). The few already edited cells at the transitional stage in $V_H3609t \times V_k21\text{-}5Tg.Thy^{KO}$ mice showed lower Rag levels than nonedited ATA B cells, similar to ATAμκTg mice under Thy^{WT} conditions (Fig. 4 B). Thus, in addition to early Rag down-regulation after exiting from the BM and before entering the spleen, the BCR editing capacity continues in the spleen at the transitional stage.

To examine whether BCR-engaged signaling leads to Nod1 up-regulation, purified FO B cells from WT mice were stimulated with anti-IgM in vitro (Fig. 4 C). This in vitro culture data did not show direct Nod1 up-regulation by anti-IgM or by LPS or CpG TLR stimulation (Fig. 4 C), regardless of the presence or absence of BAFF. Also, naive ATA B cells in the spleen (transitional B and FO B cells) stimulated with Thy^{M} antigen did not show Nod1 up-regulation (unpublished data). In contrast, acute temporal induction of Ptpn22 (protein tyrosine phosphatase nonreceptor 22) mRNA occurred as an immediate consequence of BCR signaling (Fig. 4 C). For T cells, TCR stimulation also up-regulates Ptpn22, and Ptpn22 functions as a negative regulator of TCR signaling (Cohen et al., 1999; Mustelin et al., 2005). During B cell development, Ptpn22 mRNA was up-regulated at transitional stages and was higher in MZ B cells, with the highest levels in B1a B cells, including protein levels (Fig. 4 D). This indicated that BCR signaling does not directly lead to Nod1 up-regulation in vitro, in contrast to Ptpn22.

In vivo, B cells are constantly interacting with the microenvironment, and the generation of MZ B cells requires Notch2 signaling triggered by interaction with delta-like 1, which is dominantly expressed by splenic endothelium (Tan et al., 2009). Thus, Nod1 up-regulation may also have occurred by interaction with non–B cells as a consequence of increased cell adhesion by a BCR-initiated signal (Wen et al., 2005a; Arana et al., 2008). To provide an in vivo microenvironment, nonediting ATAμκTg.Thy^{KO} mice were bred with *lck*-Thy-1 transgenic mice that express self-antigen at lower than physiological levels (intermediate in "Thy 60" or lowest in "Thy 10"; Wen et al., 2005a; Fig. 4 E). Lower levels of Thy-1 prevent a maturation arrest and instead yield early maturating FO B cells (by Thy 60) or matured FO B cells together strongly with MZ B cells (by Thy 10), without BCR editing (Wen et al., 2005a). As shown in Fig. 4 E, the level of Nod1 in ATA FO B cells from such mice was higher than in self-antigen unexposed ATA B cells in littermates, paralleling Ptpn22 mRNA levels. This result indicated that BCR engagement directly induces Ptpn22 up-regulation, followed by Nod1 up-regulation in a physiological microenvironment in vivo (Fig. 4 E, right). The lowest (nearly undetectable) Ptpn22 protein level in WT FO B cells (Fig. 4 D) is likely caused by weak BCR signaling, transient Ptpn22 up-regulation, and loss by degradation. This secondary induction of Nod1 in vivo does not involve CD40 signaling or follicular dendritic cells (Fig. 4 F). In lymphotoxin α–deficient ($LT\alpha^{-/-}$) mice, the generation of follicular dendritic cells and B cell follicle formation are defective, whereas mature B cells are generated and increase in the circulation (De Togni et al., 1994). Thus, BCR signal–initiated Nod1 up-regulation occurs independently of T cell–CD40 signaling and in the absence of follicle formation.

In edited $V_H3609t \times V_k21\text{-}5Tg$ mice, both Nod1 and Ptpn22 mRNA were expressed at higher levels by arrested ATA B cells under Thy^{WT} conditions when compared with transitional ATA B cells in Thy^{KO} mice (Fig. 4 G), confirming Nod1 and Ptpn22 induction by self-antigen exposure. In contrast to the peak expression of Ptpn22 at the arrested stage in Thy^{WT} mice, edited B cells that became mature FO B cells expressed increased Nod1 levels compared with transitional stage on both Thy^{WT} and Thy^{KO} backgrounds, suggesting additional cell stage context dependence after BCR editing. Based upon these data, we conclude that BCR editing first provides B cells with the capability to experience BCR ligand signaling, followed by Nod1 up-regulation, generating the mature FO B cell pool, together with nonedited naive ATA B cells (Fig. 4 H).

Nod1 signaling in BCR-engaged B cells promotes mature B cell survival

We next asked whether Nod1 up-regulation by mature B cells plays a positive function in their activation and survival. FO B cells in normal mouse spleen were sensitive to stimulation with CiE-DAP (Fig. 3 E), and their survival was promoted, synergizing with BAFF (Fig. 5 A), in the absence of proliferation. Nod1 and BCR coengagement also enhanced

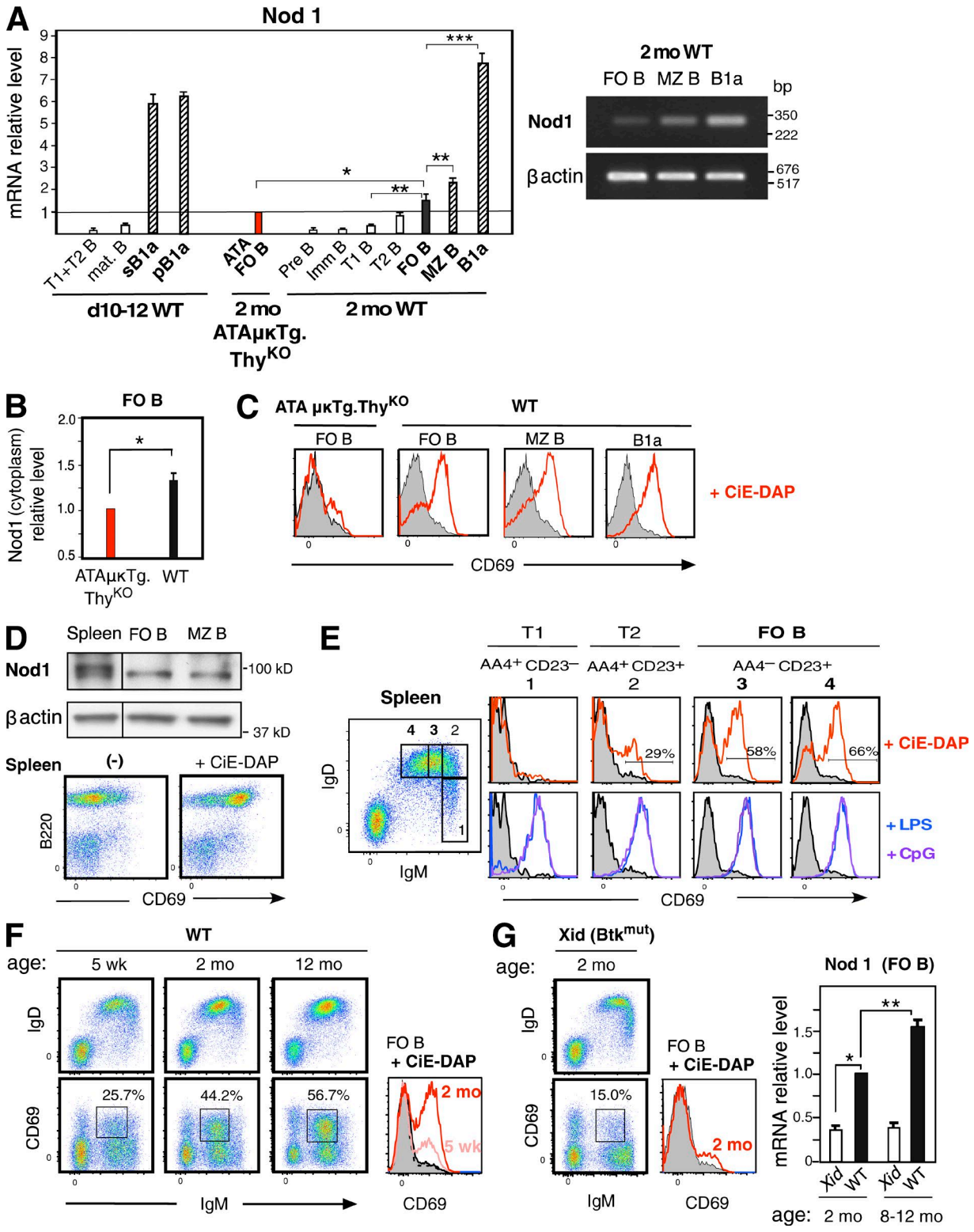

Figure 3. **Nod1 ligand signal–sensitive mature B cells increase with age in comparison to *Xid* mice.** (A) Nod1 quantitative PCR in WT neonatal and adult B-lineage cells relative to self-antigen–unexposed adult ATA FO B cells from ATAμκTg.Thy^{KO} mice (ATA FOB. Thy^{KO}), set to 1 (n = 3–5, each group; mean ± SE; *, P < 0.05; **, P < 0.01; ***, P < 0.001). mat B, mature B; pB1a, PerC B1a; sB1a, spleen B1a. Right: Nod1 RT-PCR. (B) Anti-Nod1 cytoplasmic staining level comparison between ATA FO B.Thy^{KO} cells and WT FO B cells (n = 5; mean ± SE; *, P = 0.01). (C) CiE-DAP reactivity comparison between ATA FO B.Thy^{KO} and WT mouse B cell subsets (representative of n = 4 each). (D) Top: Western blot of Nod1. Bottom: CiE-DAP–stimulated spleen cells in culture for 6 h. (E) Spleen cells

survival of all B cell subsets in normal mice in vitro, but not proliferation/CFSE dilution (Fig. 5 B). Simultaneous stimulation by CiE-DAP and anti-IgM led to increased FO B cell activation and survival. Stimulation by anti-IgM alone of MZ B or B1a B cells resulted in low or undetectable CD69 induction, respectively, and most MZ B cells died after such treatment in vitro (Oliver et al., 1999). In sharp contrast, addition of Nod1 ligand prevented MZ B death (Fig. 5 B, day 3) and further increased survival when combined with BAFF (not depicted). B1a cells, which express high Nod1 and Ptpn22 levels, showed the highest spontaneous survival in culture. Simultaneous Nod1 and BCR signaling also slightly enhanced survival relative to BCR signaling alone by B1a, without inducing proliferation.

To further assess the function of Nod1 by B cells experienced with BCR signaling, ATAμκTg.Thy^{KO} (auto^{-}), WT, and AGcAμκTg (auto^{+}) mice were compared (Fig. 5 C). In auto^{+} AGcAμκTg mice, FO and MZ AGcA B cells showed increased Nod1 and Ptpn22 expression (Fig. 5 C, 3 and 4) relative to FO B cells in auto^{-} ATA B and WT mice (Fig. 5 C, 1 and 2). Although auto^{-} FO B cells had the lowest levels of Nod1 expression, CiE-DAP still stimulated some increase in their survival, and WT FO B cells showed further increased cell survival (Fig. 5 D), with a slight increase in cell size, as seen in auto^{+} B cells (Fig. 5 D, day 3, thin lines), mediated through Nod1–Ripk2 signaling (Hasegawa et al., 2008; Fig. 5 E). Under BCR stimulation alone, although auto^{+} AGcA FO B cells were initially activated (Fig. 5 D, 6 h), activation was handicapped, resulting in diminished viability, and this deficit was more severe in MZ B cells (Fig. 5 D, day 3, thick blue lines) without BAFF. This BCR signaling handicap in auto^{+} B cells was partially rescued by Nod1 co-stimulation, resulting in activation (Fig. 5 D, day 3, blue dotted lines) and decreased cell death. Thus, Nod1 signaling exerts a positive influence on B cells by promoting antigen activation by FO B cells and survival of BCR ligand experienced B cells, including B cells with detectable autoreactivity.

NF-κB, MAPK, and PI3K activation by Nod1

NF-κB signals are essential for mature B cell persistence and function in both BCR- and BAFF-mediated survival pathways (Stadanlick et al., 2008; Cancro, 2009; Mackay and Schneider, 2009; Kurosaki et al., 2010; Mackay et al., 2010). PI3K signaling also plays a critical role. In absence of the BCR, provision of a PI3K–Akt–FoxO1 signal, rather than the IKKβ canonical NF-κB signal, promoted B cell survival (Srinivasan et al., 2009). Thus, Nod1-mediated NF-κB, MAPK, and PI3K signaling was examined. Consistent with nonlymphoid cell signaling through Nod1 (Chen et al., 2009), CiE-DAP stimulation of FO B cells in WT mice resulted in phosphorylation and degradation of IκBα (Fig. 6 A). Receptor interacting serine/threonine kinase 2 (Ripk2/Rip2) is a critical adaptor protein that is recruited by oligomerized Nod1, followed by ubiquitination and TAK1 recruitment and NF-κB activation (Hasegawa et al., 2008). In accordance, B cell Nod1-dependent NF-κB activation was Ripk2 dependent (Fig. 6 A). Nod1 stimulation of B cells also initiated MAPK activation (Chen et al., 2009; Fig. 6 B). Similar to BAFF treatment of B cells (Patke et al., 2006; Mackay and Schneider, 2009), Nod1-dependent Akt phosphorylation also occurred (Fig. 6 C) through a PI3K signaling pathway (Fig. 6 D), leading to FoxO1 and Gsk3β phosphorylation (Fig. 6 E).

To understand the functional outcome in Fig. 5 D, Nod1 signal–mediated IκBα degradation was compared in FO B and MZ B samples used in Fig. 5 D, including B1a (Fig. 6 F). Also, activation of NF-κB, Akt, and MAPK by Nod1 and/or anti-IgM stimulation was compared and summarized in Fig. 6 G (time-course analysis is shown in Fig. S4). CiE-DAP treatment alone increased NF-κB signaling with IκBα down-regulation and Akt phosphorylation in all Nod1–up-regulated auto^{+} B cells and WT FO B cells compared with auto^{-} FO B cells. CiE-DAP–treated auto^{-} FO B cells also lacked JNK and Erk phosphorylation but showed low-level p38 MAPK phosphorylation. Conversely, with BCR cross-linking alone, both auto^{-} and WT FO B cells induced NF-κB, Akt, and MAPK signals. In contrast, these BCR-induced signals were weaker or lacking in auto^{+} B cells, reflecting an anergic/tolerant state. Simultaneous BCR and Nod1 activation of FO B cells from WT mice consistently showed further increased NF-κB and JNK signals compared with auto^{-} FO B cells, leading to greater activation and survival as found in Fig. 5 B. For auto^{+} B cells, induction of NF-κB, Akt, and JNK activation was consistently high upon engagement of Nod1 alone or combined Nod1/BCR (Fig. 6 G), consistent with rescue from cell death or enhanced survival. Thus, after BCR signaling in vivo, the Nod1 signaling potentiates survival through a mechanism that includes NF-κB and PI3K signaling pathways, which are known for their role in B cell persistence.

Increased Nod1 in transduced B cells allows continued survival in aged mice

To assess whether Nod1 signaling is playing a role for B cells in a normal environment, we first retrovirally transduced

stimulated with CiE-DAP, LPS, CpG, or medium alone (gray). Gating was based on IgM and IgD levels, together with AA4/CD93 and CD23. CiE-DAP–induced CD69^{+} cell frequency is shown. C.B17 mouse data were similar to B6 data (two mice each). (F) CiE-DAP–stimulated spleen cells from different-aged mice were stained with IgM, IgD, and CD69, and the frequency of CD69^{+}-activated cells among IgM$^{med/lo}$IgD^{hi} FO B cells (square region) is shown. Purified 5-wk and 2-mo FO B cells stimulated with CiE-DAP (right). C.B17, BALB, and C57BL/6 mice (three mice or more each) were analyzed, confirming similar results; data from C.B17 mice are shown. (G) Spleen and purified FO B cells in 2-mo-old *Xid* mice stimulated with CiE-DAP (left and middle). Nod1 quantitative PCR of *Xid* compared with WT mouse FO B cells (right; $n = 3$ each; mean ± SE; *, $P < 0.003$; **, $P < 0.008$).

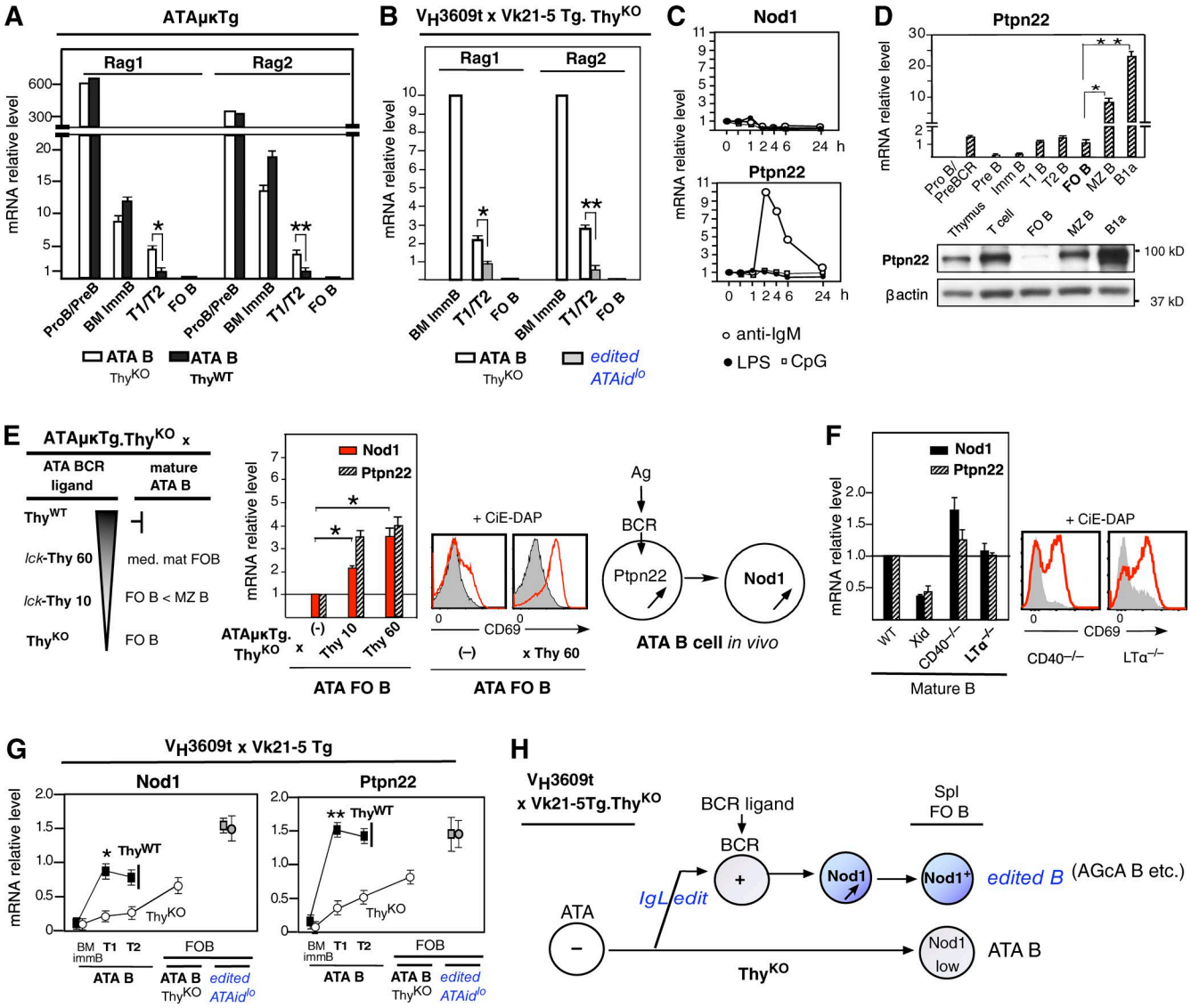

Figure 4. **Nod1 up-regulation in BCR engaged B cells in vivo.** (A) Rag1 and Rag2 quantitative PCR of ATA B cells under Thy^{KO} and Thy^{WT} in ATAμκTg mice ($n = 3$; mean ± SE; *, P = 0.03; **, P = 0.003). (B) Rag1 and Rag2 quantitative PCR of ATA B cells and edited $ATAid^{lo}$ B cells in $V_H3609t \times V_k21\text{-}5Tg.Thy^{KO}$ mice ($n = 3$; mean ± SE; *, P = 0.1; **, P = 0.03). (C) Quantitative PCR of WT (C.B17) FO B cells stimulated with anti-IgM, LPS, or CpG during 24-h culture. Similar data were obtained by B6 FO B cell simulation (two samples each). (D) Ptpn22 quantitative PCR in B-lineage cells ($n = 3$–5, each group; mean ± SE; *, $P < 0.01$; **, $P < 0.002$) and Western blot. (E) Nod1 and Ptpn22 quantitative PCR of $ATAid^+$ FO B cells sorted from $ATAμκTg.Thy^{KO}$ mice exposed to *lck*-Thy-1 Tg cells, Thy 10, or Thy 60 by breeding ($n = 3$ each, 2–3 mo old; mean ± SE; *, $P < 0.05$), comparing $ATAid^+$ FO B cells without *lck*-Thy-1 Tg, as (—) 1.0, and Thy-1 Tg^+ in littermates. CiE-DAP reactivity comparison by $ATAid^+$ FO B cells without (—) and with *lck*-Thy 60 Tg littermates (middle). Ptpn22 up-regulation resulting from a BCR ligand signal, followed by Nod1 up-regulation, occurred in vivo (right). (F) Mature ($AA4^-CD21^{med}CD23^+$) B cell Nod1 and Ptpn22 mRNA comparison ($n = 3$ each; mean ± SE). WT mice used for comparison with $LT\alpha^{-/-}$.B6 mice were B6. CiE-DAP reactivity by mature B cells in $CD40^{-/-}$ and $Lt\alpha^{-/-}$ mice (right). (G) Comparison of Nod1 and Ptpn22 mRNA levels in immature stages of ATA B cells from $V_H3609t \times V_k21\text{-}5$ Tg mice on Thy^{WT} (black square) and Thy^{KO} (open circle) backgrounds, and mature edited FO B cells (gray; $n = 4$; mean ± SE; *, $P < 0.005$; **, $P < 0.01$ for T1 comparison). (H) Edited B cells with Nod1 up-regulation as the outcome of BCR ligand engagement.

BM with Nod1-GFP. Nod1-GFP–transduced BM from nonedited auto⁻ATAμκTg.Thy^{KO} mice or edited $V_H3609t \times V_k21\text{-}5Tg.Thy^{KO}$ mice was transferred into Thy^{KO} recipients. After ATAμκTg.Thy^{KO} BM transfer, the representation of an initially small portion of Nod1-GFP^+ immature ATA B cells was strongly increased among mature ATA B cells at 3 wk in PBL and spleen FO B cells at 6 wk compared with T1 stage cells (Fig. 7 A). Thus, comparing Nod1-GFP^+ and GFP^- cells with identical ATA BCR in the same mouse confirmed that Nod1 plays a functional role in enriching the representation

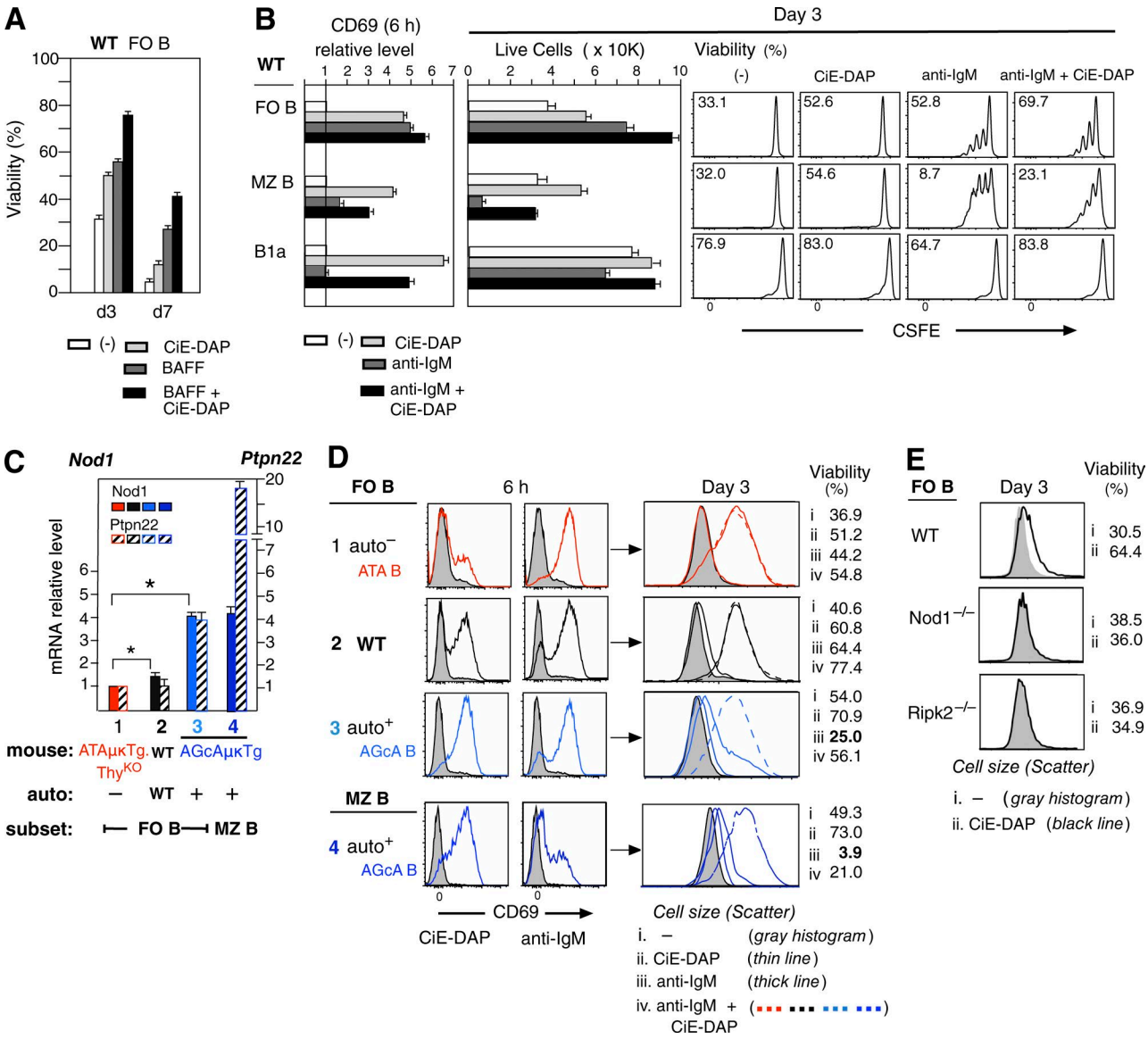

Figure 5. **Nod1 signaling promotes survival of BCR ligand–experienced B cells.** (A) Viability of FO B cells, 3 and 7 d in culture, stimulated with CiE-DAP, BAFF, or both. Total cell numbers were similar (n = 3, mean ± SE). Data obtained in C57BL/6 mouse FO B cells were similar (two samples). (B) Analysis at 6 h and 3 d after stimulation of purified B cell subsets from WT mouse. After 6 h, comparison of CD69 level by PE-anti-CD69 staining (PE mean level). For 3-d analysis, CSFE labeling of purified B cells was used for analysis of cell division and viability (%). Representative data (C.B17 mice) from seven experiments with C.B17 and BALB/c, and five experiments with C57BL/6 are shown. All showed increased viability with CiE-DAP (n = 2, mean ± SE). (C) Nod1 and Ptpn22 mRNA comparison between (1) ATA FO B from ATAμκTg.Thy^{KO} mice (auto$^-$), (2) FO B cells from WT mice, and (3 and 4) AGcA FO B and MZ B cells from AGcAμκTg mice (auto$^+$), respectively (all on a C.B17 background; n = 3 each; mean ± SE; *, $P < 0.05$). (D) B cells, listed in C, were stimulated for 6 h to 3 d by CiE-DAP (thin line), anti-IgM (thick line), and CiE-DAP plus anti-IgM (dotted line). On day 3, cell size (flow cytometry scatter) and percent viability were determined. Four experiments showed similar results. (E) Increased viability and cell size by CiE-DAP stimulation through the Nod1–Ripk2 signal in WT (B6) FO B cells.

of mature B cells (Fig. 7 B). When Nod1-GFP transduced V_H3609t xV_k21-5Tg.Thy^{KO} BM was transferred, this also resulted in increased Nod1-GFP$^+$ cells in FO B and MZ B cells (Fig. 7 C, left). Further, BCR editing was greatly reduced in mature Nod1-GFP$^+$ B cells, compared with GFP$^-$ B cells in the same mouse, and mature GFP$^+$FO B cells were predominantly ATA B cells (Fig. 7 C). In conclusion, cells with a BCR that lacks self-ligand survived in the absence of BCR editing when Nod1 was constitutively provided by retroviral transduction.

To assess potential alteration with age, PBLs of mice transferred with Nod1-GFP V_H3609t × V_k21-5Tg.Thy^{KO}

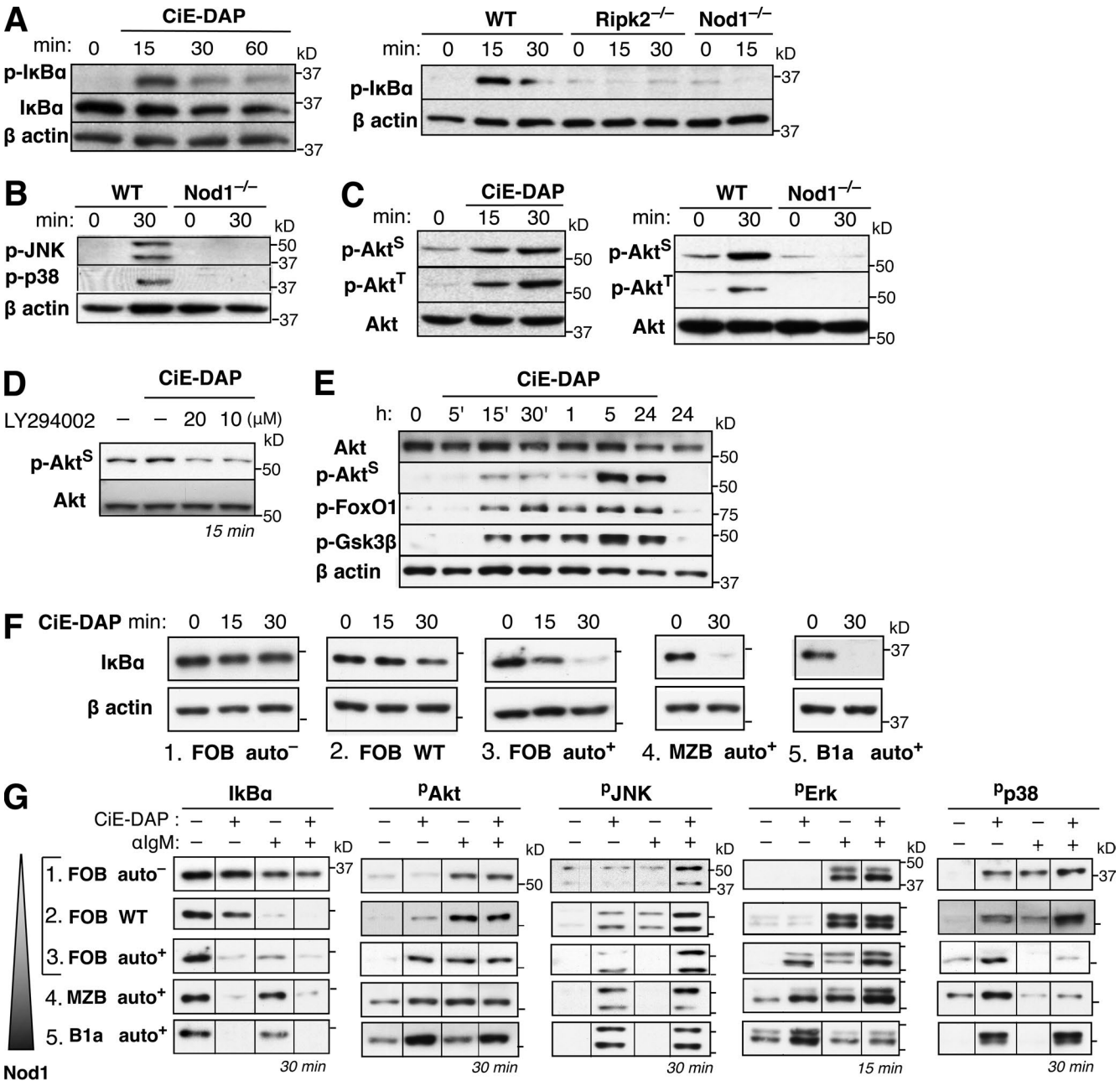

Figure 6. **Nod1-mediated NF-κB, PI3K, and MAPK signals in B cells.** (A) Western blot of WT (B6) mouse (left) and WT, Ripk2$^{-/-}$, and Nod1$^{-/-}$ FO B cells (right) stimulated with CiE-DAP, showing Nod1- and Ripk2-dependent IκBα phosphorylation. (B) Activation of MAPK by CiE-DAP stimulation. (C) Nod1-dependent Akt Ser473/Thr308 phosphorylation in CiE-DAP–stimulated FO B cells. (D) The PI3K inhibitor LY294002 inhibits Akt phosphorylation induced by CiE-DAP stimulation. (E) FO B cell stimulation with CiE-DAP from 5 min to 24 h, and kinetic analysis of phosphorylated Akt, FoxO1, and Gsk3β. Initial phosphorylated Akt was transient, declining after 1 h and then recovering. (F) Comparison of CiE-DAP–mediated Nod1 signal–induced IκBα degradation in different B cell subsets. Samples 1–4 were the same as in Fig. 5 D (1–4). Sample 5 was autoreactive B1a from V_H11 knock-in mice (auto$^+$; Wen et al., 2005b) and the lowest (or negative) by auto$^-$ FO B cells. (G) Summary of Western blot results of Nod1, BCR, and Nod1-BCR signaling of FO B, MZ B, and B1a B cells. β-Actin levels were all similar within each Western blot. Nod1-BCR co-stimulation consistently increased the NF-κB and JNK signal for WT FO B cells and overrode autoreactive B cell tolerance. Shown are representative data from two to three experiments for each B cell stimulation.

BM were monitored for 12 mo (Fig. 7 D). As expected, GFP$^-$ cells had a higher number of edited B cells (as originally found; Fig. 2 F). In contrast, ATA B cells were consistently dominant among Nod1-GFP$^+$ B cells. Although the number of edited B cells slightly increased among GFP$^+$ cells with age, these cells expressed a lower level of GFP than

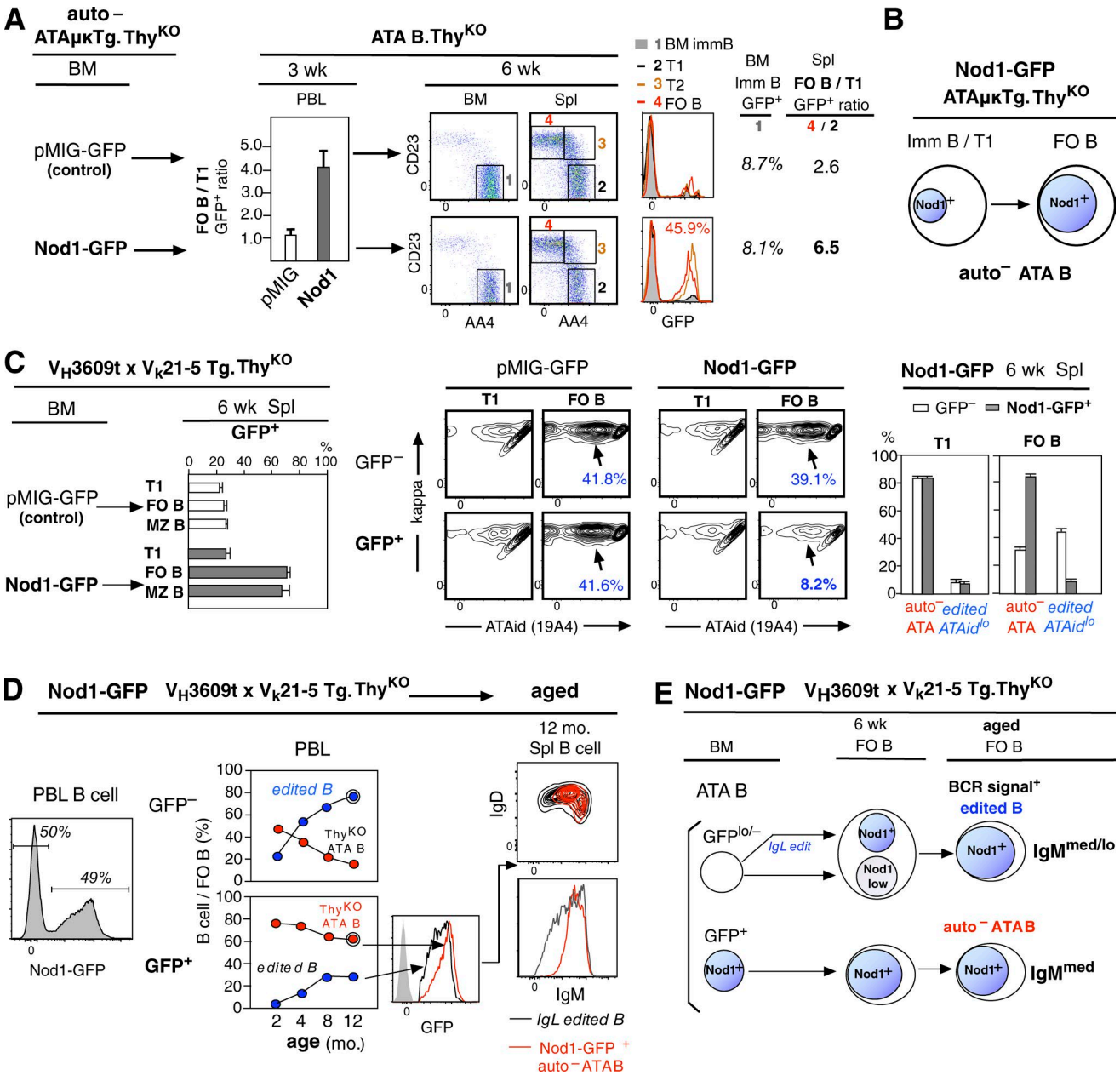

Figure 7. **Continued B cell survival in aged mice by transduced Nod1 expression.** (A) Transfer of nonedited auto⁻ATAμκTg.Thy^{KO} mouse BM with Nod1-GFP or pMIG (without Nod1)-GFP as a control. Comparison of GFP$^+$ cell frequency in ATA B cells between the FO B cell and T1 stage (as a ratio) in PBLs at 3 wk (n = 6 each; mean ± SE) and spleen at 6 wk. In the 6-wk GFP histogram, immature B cells in BM (1) are shown in gray, along with GFP$^+$ frequency. Data are representative of n = 6 each. (B) Increase in the number of Nod1-GFP$^+$ cells in the ATA FO B cell pool under Thy^{KO}. (C) Transfer of edited V_H3609t × V_k21-5 Tg.Thy^{KO} mouse BM with Nod1-GFP or control-GFP into Rag^{KO}Thy^{KO} recipients. Spleen B cell analysis 6 wk after transfer, comparing GFP$^+$ and GFP$^-$ B cell subsets, with percentage of edited ATAid^{lo} cells (middle). Nod1-GFP transfected B cell data (right; n = 3 each; mean ± SE). (D) PBL B cell analysis during aging (and spleen in aged mice) after transfer with Nod1-GFP V_H3609t × V_k21-5 Tg.Thy^{KO} mouse BM. After transfer, the WT/knockout mouse B cell ratio levels in spleen were based on the WT/knockout mouse B cell ratio level data of T1 (CD19$^+$IgM^{hi}AA4$^+$CD21$^-$CD23$^-$ as 1.0. IgM/IgD phenotype of GFP$^+$ B cells (right). Unchanged IgM^{med} level by Nod1-GFP$^{+\,hi}$ auto⁻ATA B cells 12 mo after transfer, in comparison with edited GFP$^{+\,med}$ B cells with IgM^{lo} B cells. Data are representative of three recipients. (E) Increased survival outcome by FO B cells in aged mice by Nod1 up-regulation. IgM^{lo}IgD$^+$ FO B cells are predominantly BCR signal–experienced Nod1$^+$ B cells.

nonedited GFP$^+$ ATA B cells (Fig. 7 D, middle). Also, GFP^{hi+} nonedited ATA B cells continued to be IgM^{med}IgD$^+$ B cells, unlike edited B cells (GFP$^{lo/-}$), which included IgM^{lo}IgD$^+$ B cells. This confirmed an increased survival outcome of Nod1$^+$ B cells in aged mice and suggested that IgM^{lo}IgD$^+$ FO B cells are predominantly BCR signal–experienced Nod1-up-regulated B cells (Fig. 7 E).

Competitive survival of mature B cells promoted by Nod1–Ripk2 signaling

In contrast to Nod1-GFP, reduction of Nod1 by shNod1-GFP transduction in auto$^+$ AGcATg BM resulted in decreased representation among AGcA FO B cells relative to transduction with empty-vector GFP$^+$ control (Fig. 8 A). These GFP experiments confirmed that Nod1 signaling is playing a functional role in enriching or depleting the representation of mature B cells, depending on its level of expression. However, in Nod1-deficient (Nod1$^{-/-}$) mice, mature B cell subset generation occurs. Because NLR Nod2 was found in B1a cells and at lower levels in MZ B and FO B cells (Fig. S5 A), there was a possibility that Nod2 signaling was compensating in Nod1$^{-/-}$ mice. Thus, we tested Nod1 and Nod2 double-knockout mice (Nod1/2$^{-/-}$) and Ripk2$^{-/-}$ mice, both of which have defective Nod1 and Nod2 signaling. However, both Nod1/2$^{-/-}$ (Fig. 8 B) and Ripk2$^{-/-}$ (Fig. 8 C) mice showed B cell generation similar to WT and Nod1$^{-/-}$ mice. Importantly, we found that mature FO B cells in Ripk2$^{-/-}$ mice had Nod1$^+$ and Ptpn22$^+$ mRNA levels similar to those from Ripk2$^{+/+}$ littermates, and BCR signaling was normal (Fig. 8 C). These results indicated that the Nod1 signaling is not required in the initial generation and maturation of BCR-engaged B cells with Nod1 up-regulation.

Because both Nod1 up-regulated and non–up-regulated B cells mature and survive in the presence of BAFF, a possible role for Nod1 signaling in normal mice was competitive survival, considering our auto$^-$ and auto$^+$ B cell GFP transduction data. Thus, we performed 1:1 mixed BM chimeric transfer from WT (Ly5.1) and Nod1/2$^{-/-}$(Ly5.2) mice. Compared with B cells at the transitional stage ("1"; IgM^{hi} IgD^{lo} AA4$^+$), the WT to Nod1/2$^{-/-}$ B cell ratio was slightly but consistently increased in mature B cells in PBLs and in FO B and MZ B cells in the spleen (Fig. 8 D). Thus, the frequency of Nod1/2$^{-/-}$ B cells decreased with maturation. When BM cells from Ripk2$^{-/-}$ mice were cotransferred with WT, increased competitive survival of Ripk2$^+$ (WT) FO and MZ B cells also occurred (Fig. 8 E), including a higher WT/Ripk2$^{-/-}$ ratio by MZ B lineage.

In the absence of competitive B cells, Ripk2 deficiency in auto$^+$AGcAμκTg mice also did not affect AGcA B cell maturation (Fig. 8 F). When WT BM cells were cotransferred at a three times greater frequency than AGcA BM cells, Ripk2$^{+/+}$AGcA B cells became the preferred CD21^{hi} B cell type entering the MZ B subset (Fig. 8 G, top), as previously observed (Ichikawa et al., 2015). In contrast, generation of Ripk2$^{-/-}$ AGcA B cells was significantly reduced with limited MZ B cell generation (Fig. 8 G, bottom). LPS- and CpG TLR-mediated proliferation was normal in Ripk2$^{-/-}$ AGcA B cells, whereas Ripk2 deficiency blocked rescue from BCR signal–mediated death upon Nod1 ligand addition (Fig. S5 B). Thus, it is clear that a Nod1–Ripk2 signaling is occurring in Nod1$^+$ B cells, and an intact Nod1 signal confers a competitive advantage for both FO B and MZ B cell generation and maintenance.

Chimeric transfers of purified splenic B cells also revealed a gradual increase of Rip2$^{+/+}$ WT B cells over Ripk2$^{-/-}$ B cells in PBLs (Fig. 8 H). 12 wk posttransfer, after 40–50% B cell loss, 20–30% of the surviving B cells in circulation and the spleen were IgM^{hi}IgD^{lo} AA4$^-$ (with up-regulated Blimp1; not depicted) and predominantly Ripk2$^{+/+}$ (Fig. 8 H). This confirmed that a physiological Nod1 ligand interacts directly with responsive B cells, and the Nod1–Ripk2 signal promotes competitive survival for BCR-engaged Nod1–up-regulated B cells, including edited B cells (Fig. 8 I).

DISCUSSION

Our data demonstrate that Nod1 up-regulation has a positive impact on BCR-engaged mature B cells. Exposure of the BCR to self-ligands is a critical event that impacts B cell development. Through B-2 development, antigen-unexposed naive B cells can become mature FO B cells when sufficient BAFF is provided. Such naive B cell maturation without BCR ligand signaling was confirmed in our ATA knock-in mouse system. However, we also observed an increase in BCR-edited B cells that predominated with age. We show here that these edited mature B cells up-regulate Nod1 as an outcome of BCR engagement in vivo. Although Nod1 up-regulation also occurs at the arrested stage during negative selection, mature B cells express even higher Nod1 mRNA levels and Nod1 ligand responsiveness. This indicates that Nod1 up-regulation is cell stage context dependent and only reaches functional levels at the mature cell stage in vivo. A positive outcome by increased Nod1 was confirmed by transduction, and up-regulation of Nod1 in normal mice promotes competitive survival by mature B cells.

Nod1 signaling does not require initial BCR-engaged mature B cell generation. This BCR-engaged Nod1$^+$ mature B cell generation might be due to either altered BCR sensitivity of mature B cells in sensing their microenvironment and/or increased simultaneous signaling by BCR ligand and BAFF as an initial positive outcome. It is after such BCR-engaged mature B cell generation that the NLR signal begins to play a role. The presence of Nod1 ligand, a commensal microbial product, promotes B cell survival, synergizing with BAFF and conferring an advantage relative to B cells lacking BCR-ligand exposure. Thus, the FO B and MZ B cell subsets become further enriched for B cells with NLR signaling capacity. Our finding of an initial BCR ligand signal, followed by a secondary Nod1 signal promoting competitive survival, explains the importance of canonical NF-κB and PI3K signal involvement for FO B cell generation and

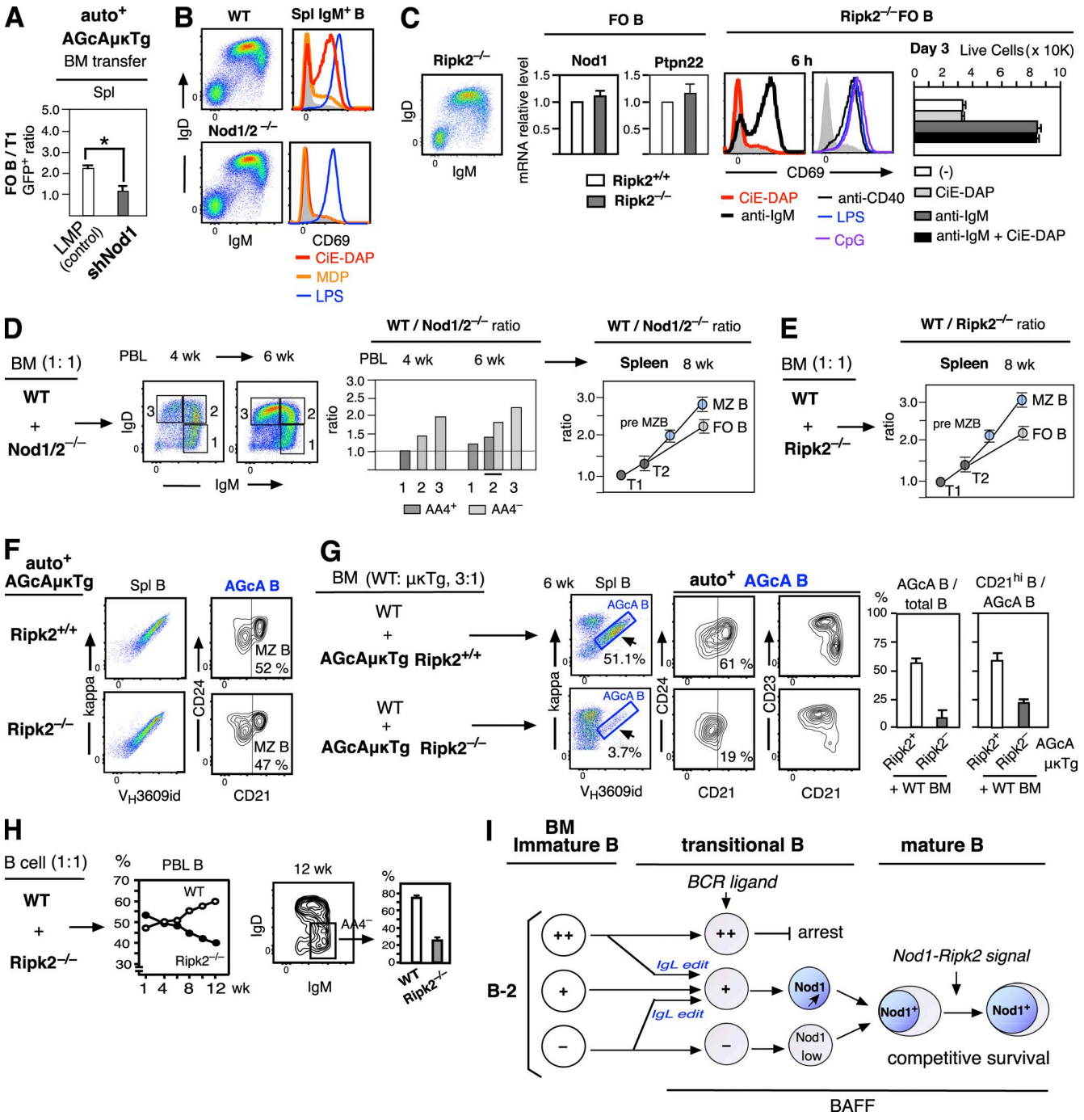

Figure 8. **Competitive survival by mature B cells promoted by Nod1–Ripk2 signaling.** (A) FO B/T1 GFP$^+$ AGcA B cell ratio in spleen 5–6 wk after transfer of AGcATg mouse BM with shNod1-GFP or LMP (without shNod1)-GFP as a control (n = 3 each; mean ± SE; *, P = 0.008). (B) Spleen cell analysis (IgM/IgD) and stimulation with CiE-DAP, muramyl dipeptide (Nod2 ligand), and LPS, comparing WT (B6) and Nod1/2$^{-/-}$ mice. (C) Ripk2$^{-/-}$ mouse FO B cell Nod1 and Ptpn22 levels in comparison with Ripk2$^{+/+}$ littermates (middle; quantitative PCR; n = 3 each; mean ± SE). Ripk2$^{-/-}$ FO B stimulation analysis (right). (D) Chimeric transfer of WT (Ly5.1) and Nod1/2$^{-/-}$ (Ly5.2) mouse BM at a 1:1 ratio. Initial (4 wk) chimeric transfer ratio was set to 1:1 at the IgM$^+$IgD^{lo}AA4$^+$ transitional cell stage ("1") in PBL. In spleen, the WT/Nod1/2$^{-/-}$ ratio was based on the T1 in each mouse (n = 3; mean ± SE). (E) Chimeric transfer of WT and Ripk2$^{-/-}$ mouse BM, as done with Nod1/2$^{-/-}$ mice in D (n = 4; mean ± SE). (F) Splenic B cells in AGcAμκTg.B6 mice without or with Ripk2 deficiency. Similar AGcA B cell dominance per number and CD21^{hi} MZ B cell frequency. Representative of three mice each. (G) Chimeric transfer of WT (B6) and AGcAμκTg (Ripk2$^{+/+}$ or Ripk2$^{-/-}$) BM at a 3:1 ratio, followed by splenic B cell analysis. Frequencies of AGcA B cells (as marked, also V_k19-17 recognizing 13H8k$^+$) in total B cells and CD21^{hi} cells among AGcA B cells are shown (n = 3; mean ± SE). (H) 1:1 chimeric transfer of purified B cells from Ripk2$^{+/+}$ WT and Ripk2$^{-/-}$ mouse spleen, followed by analysis of PBL B cells and

maintenance. Although BCR-engaged selection occurs, the immune system must cope with the unlimited diversity of antibodies that B cells can generate. Because a great degree of conformational flexibility exists in the unmutated germline structure of antibodies (Wedemayer et al., 1997), the mature FO B cell pool retains great diversity as a primary repertoire.

It is still unclear how BCR signaling is involved in Nod1 up-regulation, because BCR ligand–mediated signaling does not directly induce Nod1. In vivo, developing B-2 B cells circulate from BM, entering the spleen which is the main site filtering the blood. In this process, B cells encounter the microenvironment, including serum immunoglobulins, dendritic cells, and vascular endothelial cells. Considering that BCR ligand signaling promotes cell adhesion (Wen et al., 2005a; Arana et al., 2008), interaction with nonlymphoid cells and increase of Nod1 may occur. The accumulation of Nod1 up-regulated B cells appears to be the result of a complex interplay with the microenvironment. Initially, it is likely to be dependent on the amount, form, and valency of antigen engaging the BCR, including polyvalent antigen engagement to become $IgM^{lo}IgD^{+}$ FO B cells (Übelhart et al., 2015), followed by interaction with nonlymphoid cells.

The positive influence of coexisting microorganisms on the immune system has become increasingly apparent (Mazmanian and Kasper, 2006). After birth, microbiota-mediated Nod1 signaling by epithelia can contribute to the initial maturation of isolated lymphoid follicles with B cells in intestine (Bouskra et al., 2008). Nod1 signaling through nonhematopoietic cells also strongly contributes to induction of adaptive immunity together with antigen (Fritz et al., 2007). Now, our data show that mature B cells expressing Nod1 can directly respond to Nod1 ligands. Because stimulation of cytosolic Nod1 does not require physical contact with live bacteria, and because bacterial products can circulate (Clarke et al., 2010), mature $Nod1^{+}$ B cells become sensitive to Nod1 signals. Increased sensitivity to the Nod1 ligand induces survival of B cells, but not proliferation. Thus, the increase in Nod1 in mature B cells promotes a positive survival outcome, increases BCR activation, and rescues cells from BCR-induced tolerance. Increased survival by Nod1 signaling in aged mice may also involve NLR in autophagy as a host defense by maintaining immune homeostasis (Philpott et al., 2014). An increase in autoreactive B cells with age in both mice and humans may be caused in part by continuous NLR signaling throughout life, a consequence of the presence of commensal microbiota. Although it is possible that nonautoreactive B cells also become high Nod1-expressing B cells, because the BCR signal does not directly induce Nod1, understanding the function of commensal microorganisms in enriching Nod1 up-regulated B cells that play a beneficial role and, conversely, pose a risk of autoimmune disease or cancer with aging is important and requires future investigation.

MATERIALS AND METHODS

Mice

$V_H3609/V_k21\text{-}5$ ATA and $V_H3609/V_k19\text{-}17$ AGcAμκ transgenic mouse lines (3369 as ATAμκTg and EP67 as AGcAμκTg, respectively), Thy^{KO}, *lck*-Thy-1 transgenic lines, the $V_H3609/D/J_H2$ targeted insertion (V_H3609t) line, and the $V_k21\text{-}5/J_k2$ κ Tg mouse line have all been previously described (Hayakawa et al., 2003; Wen et al., 2005a; Ichikawa et al., 2015). All Ig transgenic and V_H3609t mouse lines were backcrossed onto the C.B17 background. *Xid* mice are on a BALB/c background, and $CD40^{-/-}$ mice are on a C.B17 background. 2–3-mo-old C.B17 (or BALB/c) mice were used as WT mice in most experiments (except as noted). C57BL/6 (B6) mice, and B6.Ly5.1 mice for cotransfer, were used as WT controls in experiments with $Nod1^{-/-}$, $Nod1/2^{-/-}$, $Ripk2^{-/-}$, or $LT\alpha^{-/-}$ mice (all on a C57BL/6 background). The AGcAμκTg mouse line was also backcrossed to C57BL/6 (Ichikawa et al., 2015) and then was crossed with $Ripk2^{-/-}$ mice for cotransfer experiments. $Nod1^{-/-}$ mice were originally made by T.W. Mak (University of Toronto, Toronto, Ontario, Canada), and $Nod1/2^{-/-}$ mice were provided by R. Tsolis (University of California at Davis, Davis, CA). All animal experiments were conducted under a protocol approved by the Fox Chase Cancer Center Institutional Animal Care and Use Committee.

Flow cytometry analysis, sorting, and reagents

Multicolor flow cytometry analysis, sorting, and monoclonal antibody reagents, including rat anti–mouse Ig idiotype antibodies, P9-19A4 (anti-ATAid), and P9-10C7 (anti-V_H3609^{SM6C10} id), have been described previously (Hayakawa et al., 2003; Wen et al., 2005a; Ichikawa et al., 2015). APC-A20 and FL-104 antibodies were used for anti-CD45.1 and anti-CD45.2 staining. Analysis and sorting for B cell subsets: FO B ($B220^{-}AA4^{-}CD21^{med}CD23^{+}$), MZ B ($B220^{+}AA4^{-}CD21^{hi}CD23^{-}$), B1a ($CD19^{+}B220^{lo}CD5^{+}$).

RT-qPCR assay

Gene expression was quantitated by real-time PCR, with duplicate samples, using TaqMan assays from Applied Biosystems, an ABI 7500 real-time thermal cycler, and ABI software (Life Technologies). Relative gene expression levels were normalized using β-actin values as a standard. A minimum of three samples were used, with up to five samples (duplicate analysis for each), to determine mean, standard error, and p-value by *t* test. For B cell subset quantitative PCR, a minimum of five samples were used. Nod1 RT-PCR primer

$IgM^{hi}IgD^{lo}AA4^{-}$ cells in PBL at 12 wk ($n = 3$, mean ± SE). (I) The microenvironment, including BCR ligands, BAFF, and microbial products, plays a role in mature B cell survival. BCR ligand–mediated Nod1 up-regulation, but without maturation arrest, leads to preferential mature B cell survival as a competitive survival, increasing the $Nod1^{+}$ B cell pool with age.

set was 5′-GATTGGAGACGAAGGGGCAA-3′ and 5′-TGGCTGTGTTCTTCTGCAGT-3′.

B cell stimulation in vitro

For CD69 analysis, cell sorter–purified B cells were cultured in a 96-well U-plate at 2×10^5 cells in 150 μl medium per well, with or without stimulation. Stimulating reagents were C12-iE-DAP (InvivoGen) at 10 μg/ml, goat $F(ab')_2$ anti-IgM (Jackson Laboratories) at 10 μg/ml, LPS (Sigma-Aldrich) at 20 μg/ml, CpG (InvivoGen) at 3 μg/ml, anti-CD40 (eBioscience) at 5 μg/ml, and muramyl dipeptide (InvivoGen) at 10 μg/ml. 6 h after stimulation, CD69 expression was analyzed using PE–anti-CD69 (eBioscience). Unseparated spleen cells were also stimulated using the same conditions, then costained with reagents to define various cell types together with anti-CD69. For survival analysis after culture, total cell number, viability, and cell size were measured by flow cytometry. BAFF (Alexis) was used at 0.2 μg/ml. For dye dilution cell division analyses, purified B cells were stained with CSFE (BioLegend), followed by stimulation in culture.

Cytoplasmic staining

To determine cytoplasmic Nod1 levels, spleen cells were first surface stained to detect FO B cells, followed by cytoplasmic staining with anti-Nod1 (LSBio), or rabbit IgG (Biotech) as a control, at 1 μg/ml, detected by APC-goat anti-rabbit (Invitrogen). Relative medium stained levels in FO B cells were used for comparison.

Western blotting

For B cell subset purification for Western blot, FO B cells ($CD21^{med}CD23^+AA4^-$) and MZ B cells ($CD21^{hi}CD23^-AA4^-$) from spleen and B1a cells ($B220^{lo}CD5^+$) from the PerC were used. To purify μκTg $(IgM^a)^+$ FO B and MZ B cells on a C.B17 mouse background, anti–IgM^b antibody was added to exclude endogenous B cells. B1a cells were sorted from both the spleen and PerC of V_H11t.CB17 mice (Wen et al., 2005b). B cell subsets purified by cell sorting (2×10^6 cells per tube) were preincubated in RPMI 1640 plus 0.5% FCS medium in 0.5 ml for 6 h and then stimulated with C12-iE-DAP and/or anti-IgM. Cell lysates were subjected to 10% SDS-PAGE. The Cell signaling analysis reagents used were anti-IκBα, anti–P-IκBα (Ser32), anti-P-p44/p42 MAPK (Erk1/2; Thr202/Tyr204), anti-P-p38 MAPK (Thr180/Tyr182), anti–P-SAPK/JNK (Thr183/Tyr185), anti–P-Akt(Ser473 and Thr308), anti–P-FoxO1 (Ser256), and anti–P-GSK3β (Ser9); protein was detected using HRP anti–rabbit IgG antibody (all from Cell Signaling Technology). The inhibitor LY294002 (Cell Signaling Technology) was used. Anti–β actin (Bethyl Lab), anti-Nod1 (LSBio), and anti-Ptpn22 (Proteintech) Western blots were done without preincubation.

Production of Nod1-GFP and shNod1-GFP constructs and retroviral transduction of B-lineage progenitors for cell transfer

To produce the Nod1 pMIG-GFP construct, the mouse full-length Nod1 cDNA in the pLenti-C-mGFP lentiviral vector was obtained from OriGene (catalog no. MR211295L2). Nod1 cDNA was subcloned into the pMIG-EGFP retroviral vector by cutting the OriGene lentiviral vector with BamHI and MluI to release the Nod1 insert. The original clone had Nod1 fused to GFP, so a stop fragment containing MluI and XhoI restriction sites (synthesized by Integrated DNA Technologies; 5′-CGCGTTAAGCGGCCGCTCTCAAC-3′ and 5′-TCGAGTTGAGAGCGGCCGCTTAA-3′; both 5′-phosphorylated and duplexed) was ligated to the end of the Nod1 fragment and into the pMIG retroviral backbone, previously cut with BamHI and XhoI. The resulting retroviral construct was verified by sequencing and then used to generate retroviral supernatant by calcium phosphate–mediated transfection of Phoenix-E cells. Nod1 overexpression was verified in transduced pro–B cells by sorting GFP^+ cells and determining mRNA levels using the TaqMan quantitative PCR assay. For production of shNod1-GFP, the retroviral vector LMP from Open Biosystems was used to express the shRNAmir construct from RNA polymerase II promoters. Hairpin sequences specific for Nod1 were from the Broad Institute public TRC portal. Oligos for hairpins were synthesized and cloned into LMP following a standard protocol, selected for appropriate size, and then verified by sequence analysis.

For cell transfer, B-lineage progenitors, including hematopoietic stem cells (through "immature" B cells in the case of μκTg or V_H3609t × V_k21-5Tg.Thy^{KO} BM transfer) were purified from BM, followed by overnight culture in medium containing OP9 stromal cell line with IL-7, and then transduced with retroviral supernatant. Medium was replaced after 2–3 h, and cells were cultured for an additional 24 h; GFP levels were checked (40–60% GFP^+ in general), and then $1–3 \times 10^5$ cells per recipient were injected i.v. into recipient mice. Recipients: 6.5 Gy irradiated C.B17.Thy^{KO} mice for ATAμκTg.Thy^{KO} BM transfer, 2 Gy irradiated C.B17 $Rag1^{KO}Thy^{KO}$ mice (Wen et al., 2005a) for V_H3609t × V_k21-5Tg.Thy^{KO} BM transfer, and 2 Gy irradiated C.B17.*scid* mice for AGcAμκTg BM transfer. Initial PBL analysis was done 3 wk after transfer to check GFP levels.

Chimeric BM cell transfer

Stem/progenitor cell–enriched fractions ($CD19^-$ IgM^- $CD5^-$ and low side scatter) were sorted from BM of B6.Ly5.1 (WT) and either $Nod1/2^{-/-}$ or $Ripk2^{-/-}$ mice and cotransferred to B6.s*cid* mice (3 Gy, 1 d before) by i.v. injection (5×10^5 cells each; total of 10^6 cells per recipient). To monitor B cell origin in PBLs, a six-color antibody combination (CD45.1, CD45.2, CD19, IgM, IgD, and AA4.1) was used. No $CD19^+IgM^+$ B cells were detected in B6.*scid* recipient alone without BM transfer. After transfer, the WT/knockout mouse B cell ratio levels in spleen were based on the WT/

knockout mouse B cell ratio level data of T1 ($CD19^+IgM^{hi}AA4^+CD21^-CD23^-$) ratio as 1.0. For B cell cotransfer (WT with $Ripk2^{-/-}$), $B220^+CD5^-$ cells were purified from spleen (5×10^6 cells per recipient). For cotransfer of WT (B6) BM with AGcAμκTg ($Ripk2^+$ or $Ripk2^-$) BM, BM cells were used at a 3:1 ratio (4.5×10^5 from WT and 1.5×10^5 from AGcAμκTg per recipient). AGcA B cell generation was monitored by V_H3609id and 13H8k (recognizing V_k19-17 L chain) costaining to detect AGcA B cells (Ichikawa et al., 2015) and anti-V_H3609id together with kappa and CD19 to define total B cells. As a control, $Ripk2^{-/-}$AGcAμκTg mouse BM cells were injected at 5×10^5 cells per recipient without cotransfer.

Accession number

Original raw microarray data are available under GEO accession no. GSE101318.

Online supplemental material

Fig. S1 shows V_H3609t mouse analysis. Fig. S2 presents V_H3609t × V_k21Tg.Thy^{WT} mouse data showing strong BCR editing under Thy^{WT} and also with Nod1 up-regulation. Fig. S3 demonstrates that the Igκ-edited $ATAid^{lo}$ cells coexpress with original ATA BCR. Fig. S4 is the time-course Western blot analysis, comparing different FO B cells. Fig. S5 shows predominant Nod1 expression over Nod2 in FO B and MZ B cells and Ripk2 deficiency effect in CiE-DAP stimulated $auto^+$ AGcAμκTg mouse B cells. Table S1 lists endogenous Igκ gene usage in edited $ATAid^{lo}$ FO B cells. Table S2 presents a comparison of genes between B cells with unedited and edited BCRs in Excel format.

ACKNOWLEDGMENTS

We thank Li-Jun Wen for generation of V_H3609t knock-in mice, Alex Kowalczyk for assistance with serum ATA analysis, and several Fox Chase Cancer Center Facilities (Lab Animal, Flow Cytometry, Transgenic, and DNA Sequencing) for technical support. We also thank Renée Tsolis for providing Nod1 and Nod2 double-knockout mice and D. Kappes and K. Campbell for comments on the manuscript.

This work was supported by the National Institutes of Health (grant RO1 AI49335 to K. Hayakawa, grant AI026782 to R.R. Hardy, grant AI113320 to R.R. Hardy and K. Hayakawa, and grant DK61707 to G. Núñez) and the Fox Chase Cancer Center Blood Cell Development and Cancer Keystone program.

The authors declare no competing financial interests.

Author contributions: K. Hayakawa designed the study, performed the experiments, and wrote the manuscript. R.R. Hardy supervised mouse model generation, cloning and transduction of Nod- and shNod1-GFP BM for cell transfer, discussed the work with K. Hayakawa, and contributed to writing the manuscript. A.M. Formica performed BCR gene sequence, quantitative PCR, and Western blot analysis. Y. Zhou, supervised by Y.-S. Li, performed the microarray analysis that led to the discovery of the significance of Nod1. D. Ichikawa and M. Asano contributed original findings of AGcA B generation and determination of its specificity. J. Brill-Dashoff contributed technical help with mouse model generation, breeding, and screening. S.A. Shinton generated retroviral supernatant, transduced B cell precursors, and performed cell transfers. G. Núñez provided Nod1 knockout mice and discussed the work.

Submitted: 17 March 2017
Revised: 11 June 2017
Accepted: 24 July 2017

REFERENCES

Arana, E., N.E. Harwood, and F.D. Batista. 2008. Regulation of integrin activation through the B-cell receptor. *J. Cell Sci.* 121:2279–2286. http://dx.doi.org/10.1242/jcs.017905

Baumgarth, N. 2011. The double life of a B-1 cell: Self-reactivity selects for protective effector functions. *Nat. Rev. Immunol.* 11:34–46. http://dx.doi.org/10.1038/nri2901

Bouskra, D., C. Brézillon, M. Bérard, C. Werts, R. Varona, I.G. Boneca, and G. Eberl. 2008. Lymphoid tissue genesis induced by commensals through NOD1 regulates intestinal homeostasis. *Nature.* 456:507–510. http://dx.doi.org/10.1038/nature07450

Braun, U., K. Rajewsky, and R. Pelanda. 2000. Different sensitivity to receptor editing of B cells from mice hemizygous or homozygous for targeted Ig transgenes. *Proc. Natl. Acad. Sci. USA.* 97:7429–7434. http://dx.doi.org/10.1073/pnas.050578497

Cancro, M.P. 2009. Signalling crosstalk in B cells: Managing worth and need. *Nat. Rev. Immunol.* 9:657–661. http://dx.doi.org/10.1038/nri2621

Cascalho, M., J. Wong, and M. Wabl. 1997. VH gene replacement in hyperselected B cells of the quasimonoclonal mouse. *J. Immunol.* 159:5795–5801.

Chamaillard, M., M. Hashimoto, Y. Horie, J. Masumoto, S. Qiu, L. Saab, Y. Ogura, A. Kawasaki, K. Fukase, S. Kusumoto, et al. 2003. An essential role for NOD1 in host recognition of bacterial peptidoglycan containing diaminopimelic acid. *Nat. Immunol.* 4:702–707. http://dx.doi.org/10.1038/ni945

Chen, G., M.H. Shaw, Y.G. Kim, and G. Nuñez. 2009. NOD-like receptors: Role in innate immunity and inflammatory disease. *Annu. Rev. Pathol.* 4:365–398. http://dx.doi.org/10.1146/annurev.pathol.4.110807.092239

Clarke, T.B., K.M. Davis, E.S. Lysenko, A.Y. Zhou, Y. Yu, and J.N. Weiser. 2010. Recognition of peptidoglycan from the microbiota by Nod1 enhances systemic innate immunity. *Nat. Med.* 16:228–231. http://dx.doi.org/10.1038/nm.2087

Cohen, S., H. Dadi, E. Shaoul, N. Sharfe, and C.M. Roifman. 1999. Cloning and characterization of a lymphoid-specific, inducible human protein tyrosine phosphatase, Lyp. *Blood.* 93:2013–2024.

De Togni, P., J. Goellner, N.H. Ruddle, P.R. Streeter, A. Fick, S. Mariathasan, S.C. Smith, R. Carlson, L.P. Shornick, J. Strauss-Schoenberger, et al. 1994. Abnormal development of peripheral lymphoid organs in mice deficient in lymphotoxin. *Science.* 264:703–707. http://dx.doi.org/10.1126/science.8171322

Fritz, J.H., R.L. Ferrero, D.J. Philpott, and S.E. Girardin. 2006. Nod-like proteins in immunity, inflammation and disease. *Nat. Immunol.* 7:1250–1257. http://dx.doi.org/10.1038/ni1412

Fritz, J.H., L. Le Bourhis, G. Sellge, J.G. Magalhaes, H. Fsihi, T.A. Kufer, C. Collins, J. Viala, R.L. Ferrero, S.E. Girardin, and D.J. Philpott. 2007. Nod1-mediated innate immune recognition of peptidoglycan contributes to the onset of adaptive immunity. *Immunity.* 26:445–459. http://dx.doi.org/10.1016/j.immuni.2007.03.009

Halverson, R., R.M. Torres, and R. Pelanda. 2004. Receptor editing is the main mechanism of B cell tolerance toward membrane antigens. *Nat. Immunol.* 5:645–650. http://dx.doi.org/10.1038/ni1076

Hardy, R.R., and K. Hayakawa. 2001. B cell development pathways. *Annu. Rev. Immunol.* 19:595–621. http://dx.doi.org/10.1146/annurev.immunol.19.1.595

Hasegawa, M., Y. Fujimoto, P.C. Lucas, H. Nakano, K. Fukase, G. Núñez, and N. Inohara. 2008. A critical role of RICK/RIP2 polyubiquitination in Nod-induced NF-kappaB activation. *EMBO J.* 27:373–383. http://dx.doi.org/10.1038/sj.emboj.7601962

Hayakawa, K., M. Asano, S.A. Shinton, M. Gui, D. Allman, C.L. Stewart, J. Silver, and R.R. Hardy. 1999. Positive selection of natural autoreactive B cells. *Science.* 285:113–116. http://dx.doi.org/10.1126/science.285.5424.113

Hayakawa, K., M. Asano, S.A. Shinton, M. Gui, L.J. Wen, J. Dashoff, and R.R. Hardy. 2003. Positive selection of anti-thy-1 autoreactive B-1 cells and

natural serum autoantibody production independent from bone marrow B cell development. *J. Exp. Med.* 197:87–99. http://dx.doi.org/10.1084/jem.20021459

Hayakawa, K., A.M. Formica, J. Brill-Dashoff, S.A. Shinton, D. Ichikawa, Y. Zhou, H.C. Morse III, and R.R. Hardy. 2016. Early generated B1 B cells with restricted BCRs become chronic lymphocytic leukemia with continued c-Myc and low Bmf expression. *J. Exp. Med.* 213:3007–3024. http://dx.doi.org/10.1084/jem.20160712

Ichikawa, D., M. Asano, S.A. Shinton, J. Brill-Dashoff, A.M. Formica, A. Velcich, R.R. Hardy, and K. Hayakawa. 2015. Natural anti-intestinal goblet cell autoantibody production from marginal zone B cells. *J. Immunol.* 194:606–614. http://dx.doi.org/10.4049/jimmunol.1402383

Klein, L., M. Hinterberger, G. Wirnsberger, and B. Kyewski. 2009. Antigen presentation in the thymus for positive selection and central tolerance induction. *Nat. Rev. Immunol.* 9:833–844. http://dx.doi.org/10.1038/nri2669

Kraus, M., M.B. Alimzhanov, N. Rajewsky, and K. Rajewsky. 2004. Survival of resting mature B lymphocytes depends on BCR signaling via the Igalpha/beta heterodimer. *Cell.* 117:787–800. http://dx.doi.org/10.1016/j.cell.2004.05.014

Kurosaki, T., H. Shinohara, and Y. Baba. 2010. B cell signaling and fate decision. *Annu. Rev. Immunol.* 28:21–55. http://dx.doi.org/10.1146/annurev.immunol.021908.132541

Mackay, F., and P. Schneider. 2009. Cracking the BAFF code. *Nat. Rev. Immunol.* 9:491–502. http://dx.doi.org/10.1038/nri2572

Mackay, F., W.A. Figgett, D. Saulep, M. Lepage, and M.L. Hibbs. 2010. B-cell stage and context-dependent requirements for survival signals from BAFF and the B-cell receptor. *Immunol. Rev.* 237:205–225. http://dx.doi.org/10.1111/j.1600-065X.2010.00944.x

Martin, F., and J.F. Kearney. 2000. Positive selection from newly formed to marginal zone B cells depends on the rate of clonal production, CD19, and btk. *Immunity.* 12:39–49. http://dx.doi.org/10.1016/S1074-7613(00)80157-0

Mazmanian, S.K., and D.L. Kasper. 2006. The love-hate relationship between bacterial polysaccharides and the host immune system. *Nat. Rev. Immunol.* 6:849–858. http://dx.doi.org/10.1038/nri1956

Mustelin, T., T. Vang, and N. Bottini. 2005. Protein tyrosine phosphatases and the immune response. *Nat. Rev. Immunol.* 5:43–57. http://dx.doi.org/10.1038/nri1530

Nemazee, D. 2006. Receptor editing in lymphocyte development and central tolerance. *Nat. Rev. Immunol.* 6:728–740. http://dx.doi.org/10.1038/nri1939

Oliver, A.M., F. Martin, and J.F. Kearney. 1999. IgMhighCD21high lymphocytes enriched in the splenic marginal zone generate effector cells more rapidly than the bulk of follicular B cells. *J. Immunol.* 162:7198–7207.

Patke, A., I. Mecklenbräuker, H. Erdjument-Bromage, P. Tempst, and A. Tarakhovsky. 2006. BAFF controls B cell metabolic fitness through a PKC beta- and Akt-dependent mechanism. *J. Exp. Med.* 203:2551–2562. http://dx.doi.org/10.1084/jem.20060990

Pelanda, R., S. Schwers, E. Sonoda, R.M. Torres, D. Nemazee, and K. Rajewsky. 1997. Receptor editing in a transgenic mouse model: site, efficiency, and role in B cell tolerance and antibody diversification. *Immunity.* 7:765–775. http://dx.doi.org/10.1016/S1074-7613(00)80395-7

Philpott, D.J., M.T. Sorbara, S.J. Robertson, K. Croitoru, and S.E. Girardin. 2014. NOD proteins: Regulators of inflammation in health and disease. *Nat. Rev. Immunol.* 14:9–23. http://dx.doi.org/10.1038/nri3565

Rowland, S.L., C.L. DePersis, R.M. Torres, and R. Pelanda. 2010. Ras activation of Erk restores impaired tonic BCR signaling and rescues immature B cell differentiation. *J. Exp. Med.* 207:607–621. http://dx.doi.org/10.1084/jem.20091673

Srinivasan, L., Y. Sasaki, D.P. Calado, B. Zhang, J.H. Paik, R.A. DePinho, J.L. Kutok, J.F. Kearney, K.L. Otipoby, and K. Rajewsky. 2009. PI3 kinase signals BCR-dependent mature B cell survival. *Cell.* 139:573–586. http://dx.doi.org/10.1016/j.cell.2009.08.041

Stadanlick, J.E., M. Kaileh, F.G. Karnell, J.L. Scholz, J.P. Miller, W.J. Quinn III, R.J. Brezski, L.S. Treml, K.A. Jordan, J.G. Monroe, et al. 2008. Tonic B cell antigen receptor signals supply an NF-kappaB substrate for prosurvival BLyS signaling. *Nat. Immunol.* 9:1379–1387. http://dx.doi.org/10.1038/ni.1666

Tan, J.B., K. Xu, K. Cretegny, I. Visan, J.S. Yuan, S.E. Egan, and C.J. Guidos. 2009. Lunatic and manic fringe cooperatively enhance marginal zone B cell precursor competition for delta-like 1 in splenic endothelial niches. *Immunity.* 30:254–263. http://dx.doi.org/10.1016/j.immuni.2008.12.016

Thomas, J.D., P. Sideras, C.I. Smith, I. Vorechovský, V. Chapman, and W.E. Paul. 1993. Colocalization of X-linked agammaglobulinemia and X-linked immunodeficiency genes. *Science.* 261:355–358. http://dx.doi.org/10.1126/science.8332900

Thome, M. 2004. CARMA1, BCL-10 and MALT1 in lymphocyte development and activation. *Nat. Rev. Immunol.* 4:348–359. http://dx.doi.org/10.1038/nri1352

Übelhart, R., E. Hug, M.P. Bach, T. Wossning, M. Dühren-von Minden, A.H. Horn, D. Tsiantoulas, K. Kometani, T. Kurosaki, C.J. Binder, et al. 2015. Responsiveness of B cells is regulated by the hinge region of IgD. *Nat. Immunol.* 16:534–543. http://dx.doi.org/10.1038/ni.3141

Wardemann, H., S. Yurasov, A. Schaefer, J.W. Young, E. Meffre, and M.C. Nussenzweig. 2003. Predominant autoantibody production by early human B cell precursors. *Science.* 301:1374–1377. http://dx.doi.org/10.1126/science.1086907

Wardemann, H., J. Hammersen, and M.C. Nussenzweig. 2004. Human autoantibody silencing by immunoglobulin light chains. *J. Exp. Med.* 200:191–199. http://dx.doi.org/10.1084/jem.20040818

Wedemayer, G.J., P.A. Patten, L.H. Wang, P.G. Schultz, and R.C. Stevens. 1997. Structural insights into the evolution of an antibody combining site. *Science.* 276:1665–1669. http://dx.doi.org/10.1126/science.276.5319.1665

Wen, L., J. Brill-Dashoff, S.A. Shinton, M. Asano, R.R. Hardy, and K. Hayakawa. 2005a. Evidence of marginal-zone B cell-positive selection in spleen. *Immunity.* 23:297–308. http://dx.doi.org/10.1016/j.immuni.2005.08.007

Wen, L., S.A. Shinton, R.R. Hardy, and K. Hayakawa. 2005b. Association of B-1 B cells with follicular dendritic cells in spleen. *J. Immunol.* 174:6918–6926. http://dx.doi.org/10.4049/jimmunol.174.11.6918

Yu, W., H. Nagaoka, M. Jankovic, Z. Misulovin, H. Suh, A. Rolink, F. Melchers, E. Meffre, and M.C. Nussenzweig. 1999. Continued RAG expression in late stages of B cell development and no apparent re-induction after immunization. *Nature.* 400:682–687. http://dx.doi.org/10.1038/23287

Yuan, J., C.K. Nguyen, X. Liu, C. Kanellopoulou, and S.A. Muljo. 2012. Lin28b reprograms adult bone marrow hematopoietic progenitors to mediate fetal-like lymphopoiesis. *Science.* 335:1195–1200. http://dx.doi.org/10.1126/science.1216557

Zhou, Y., Y.S. Li, S.R. Bandi, L. Tang, S.A. Shinton, K. Hayakawa, and R.R. Hardy. 2015. Lin28b promotes fetal B lymphopoiesis through the transcription factor Arid3a. *J. Exp. Med.* 212:569–580. http://dx.doi.org/10.1084/jem.20141510

Zikherman, J., R. Parameswaran, and A. Weiss. 2012. Endogenous antigen tunes the responsiveness of naive B cells but not T cells. *Nature.* 489:160–164. http://dx.doi.org/10.1038/nature11311